PLASMA PHYSICS

S. CHATTOPADHYAY

Department of Mathematics, Sishu Bikash Academy,
Teghoria, Sonargaon, Narendrapur Station Road
(P.O. – R.K. Pally, P.S. – Narendrapur, Kolkata – 700150, West Bengal, India,
email: sankardjln@gmail.com; ORCID No. 0000-0003-4347-5762)

FAST ION-ACOUSTIC SOLITARY WAVES IN A WARM NEGATIVE ION PLASMA WITH TWO-TEMPERATURE NONISOTHERMAL ELECTRONS

Using the Sagdeev pseudo-potential formalism, the study of large-amplitude ion-acoustic compressive fast-mode solitons and fast-mode phase plane trajectories has been performed for a model plasma composed of warm positive and negative ions, warm positrons and two-temperature nonisothermal electrons. The critical phase velocity (V_c) is first obtained analytically by solving the dispersion relation under various physical conditions. Based on this analysis, the fast-mode phase velocity is subsequently identified as the velocity that not only exceeds the critical value, but also satisfies the criteria for the existence of solitary wave solutions, including all required boundary conditions. It is now observed from our model that the fast-mode phase velocity (V_F) is found after crossing a certain limit of critical phase velocity (V_c) for some chosen set of plasma parameters and finally the large-amplitude fast-mode compressive solitons and fast-mode phase plane trajectories of bounded periodic solutions are found under the variation of the stream velocities of positive and negative ions, the phase velocity, the temperatures of both ions and the concentration of negative ions.

K e y w o r d s: phase velocity, fast-mode solitary waves, two-temperature nonisothermal electron plasmas, isothermal positrons, fast-mode phase plane trajectories.

Highlights: (i) Stream velocities of positive and negative ions are considered.

(ii) Fast mode solitons are observed in warm positive and negative ions for different phase speeds satisfying the necessary condition for solitary wave solution and charge neutrality condition.

(iii) The critical phase velocity (V_c) is obtained from the dispersion relation for arbitrarily chosen set of plasma parameters satisfying the condition of solitary wave solution in our plasma model.

(iv) Phase plane trajectories determine the stability and nature of fast mode compressive solitons in our plasma model in which the interval of fast mode phase velocity (V_F) lies in $1.48 \leq V_F \leq 1.62$.

1. Introduction

Large-amplitude ion-acoustic compressive fast mode solitons in multi-ion plasmas are studied theoretically by a large number of physicists [1–13] for a

magnetized or an unmagnetized plasmas consisting of positive ions, negative ions and electrons. Solitary waves in nonequilibrium plasmas with the streaming motion were studied in [14–17]. Considering resonant particles in the kinetic approximation. Tagare [18] studied the effect of positive (σ_i) and negative (σ_j) ion temperatures on ion-acoustic solitons in a two-ion plasma having equal ion temperatures $(\sigma_i = \sigma_j)$. Considering any number of adiabatic positive and negative ion species and electrons, Verheest [19] investigated the fast ion-acoustic solitons in an unmagnetized plasma. After that, Das and Verheest [20] considered the same fast ion-acoustic solitons in a magnetized plasma with adiabatic positive and negative ion species along with isothermal electrons. Mishra *et al.* [21] studied fast and slow ion-acoustic solitons along with their amplitudes and widths for the effect of the temperatures and concentrations of different ion-species in a multicomponent plasma with negative ions. Following previous authors, Lakhina *et al.* [22] studied two-ion model plasma composed of cool and hot ions, and cool and hot electrons which models the plasma composition in the plasma sheet boundary layer region. On the other hand, Maharaj *et al.* [23] investigated the upper Mach number limitations for the ion-acoustic and electron-acoustic solitons. Studies on ion-acoustic solitons with two species of ions were found to support only positive polarity structures by Hellberg *et al.* [24] and Verheest *et al.* [25]. By extending the one-ion plasma model, Lakhina *et al.* [22] established a specific plasma model with two-temperature ions for which slow and fast ion-acoustic modes of solitons can be supported in the plasmas. The higher phase speed or fast ion-acoustic soliton is associated with the presence of the hot ions in the model. Furthermore, it was found that only positive polarity structures were found for both slow and fast ion-acoustic solitons. In this context, it is also mentioned that Nsengiyumva *et al.* [26] found out, in their paper, a range of velocities over which fast ion-acoustic solitons cannot propagate. In two-ion space plasmas for slow and fast ion-acoustic solitons, Maharaj *et al.* [27] considered the same temperature of hot ions and cool electrons but the temperature of hot electrons are hotter than the temperature of hot ions, and, in their study, they investigated that this model allows a broader applicability with sufficient justification for all adiabatic fluid species. Consequently the properties of fast ion-acoustic solitons

were discussed in a number of theoretical and experimental studies by some famous physicists [28–30].

In the past few years, there has been a considerable interest in understanding the behaviour of plasmas containing positive ions, electrons and a significant concentration of negative ions for studying fast mode solitons. In this connection, two-electron temperature distributions are very common in the laboratory, as well as in space plasmas. In that paper, the author also discussing various cases regarding the fast mode phase velocities under different conditions with the streaming motion of both positive and negative ions. The streams of positive (u_{i0}) and negative (u_{j0}) ions are very much important for determination of fast mode phase velocity (V_F) and its corresponding Sagdeev potential function $\psi(\phi)$ against electrostatic potential ϕ, as well as the fast mode phase plane trajectories $\frac{d\phi}{d\eta}$ against the electrostatic potential ϕ for the bounded periodic solutions, where η is defined by the Galilean transformation. We are trying to show the effect of streams and temperatures of both ions, the effect of velocity V and the concentration of negative ions (n_{j0}) on fast mode solitons in our plasma model.

The aim of this paper is to study the large-amplitude ion-acoustic compressive fast mode solitons in a multicomponent plasma consisting of warm positive and negative ions, warm positrons and two-temperature nonisothermal electrons by the Sagdeev pseudopotential method. The phase speeds of the linear wave modes supported by our model plasma, are obtained by the linear dispersion relation which is found from the condition of the solitary wave solution through the Sagdeev potential function $\psi(\phi)$.

The main finding of our investigation is to find out the fast mode phase velocity by which the large-amplitude ion-acoustic compressive fast mode solitons and the phase plane trajectories for the bounded periodic solutions of the fast mode solitary waves. In our plasma model, the temperature of negative ion (T_j) species may be higher or smaller than the temperature of positive (T_i) ion species for the formation of the large-amplitude solitary waves and phase plane trajectories.

The outline of this paper is described in the following ways:

In Sec. 2, the normalized basic equations with boundary conditions, charge neutrality conditions and the suitable Galilean transformation are given.

The expression for the Sagdeev potential function $\psi(\phi)$ for large-amplitude fast mode compressive solitons in two-temperature nonisothermal electron plasma is observed in this section and from the condition of the solitary wave solution, the most desired linear dispersion relation is obtained. The critical phase velocity (V_C) is then found out from the linear dispersion relation for streaming motion of ions under different situations. The fast mode phase velocity (V_F) is generally greater than the critical phase velocity (V_C) shown in this section and satisfies the condition of the solitary wave solution inequality. The fast mode phase plane trajectories for bounded periodic solutions are comprehensively discussed in Sec. 3. In Sec. 4, the entire problem connected with the fast mode phase velocity (V_F) and its corresponding large-amplitude solitary wave profiles from the Sagdeev potential function $\psi(\phi)$ against ϕ and fast mode phase plane trajectories $\frac{d\phi}{d\eta}$ against ϕ for bounded periodic solutions are both discussed in this section and are presented graphically under the variation of different plasma parameters. Concluding remarks are given in Sec. 5.

2. Basic Equations and Formulations

We consider an unmagnetized, nonrelativistic, collisionless plasma consisting of warm positive and negative ions, warm positrons and two-temperature nonisothermal electrons with density n_e comprising of the densities of low-temperature electrons n_{el} and high-temperature electrons n_{eh} and effective temperature T_{eff} consisting of hot component with temperature T_{eh} and cold component with temperature T_{el} which are followed by $T_{eh,f}$, $T_{eh,t}$ and $T_{el,f}$, $T_{el,t}$ where $T_{eh,f}$, $T_{eh,t}$ are, respectively, the temperatures of free and trapped electrons in high temperatures and $T_{el,f}$, $T_{el,t}$ are respectively the temperatures of free and trapped electrons in low temperatures. Treating all plasma constituents as adiabatic fluids, the nonlinear behavior of ion-acoustic waves in one-dimension may be described by the following set of normalized fluid equations:

$$\frac{\partial n_\alpha}{\partial t} + \frac{\partial}{\partial x}(n_\alpha u_\alpha) = 0, \qquad (1)$$

$$\frac{\partial u_\alpha}{\partial t} + u_\alpha \frac{\partial u_\alpha}{\partial x} + \frac{\sigma_\alpha}{Q_\alpha n_\alpha}\frac{\partial p_\alpha}{\partial x} + \frac{Z_\alpha}{Q_\alpha}\frac{\partial \phi}{\partial x} = 0, \qquad (2)$$

$$\frac{\partial p_\alpha}{\partial t} + u_\alpha \frac{\partial p_\alpha}{\partial x} + 3p_\alpha \frac{\partial u_\alpha}{\partial x} = 0, \qquad (3)$$

$$\frac{\partial^2 \phi}{\partial x^2} = n_e - \sum_\alpha Z_\alpha n_\alpha - n_p. \qquad (4)$$

Here $\alpha = i$, j respectively denotes the positive ions (i) and negative ions (j) with $Z_i = 1$ and $Z_j = -Z$, where Z_α is the charge of positive (negative) ions; n_α, u_α, p_α, σ_α, n_e, n_p and Q_α are respectively the normalized ion densities, ion velocities, ion pressures, temperature ratios of positive (negative) ions to electrons, concentrations of electrons, concentrations of positrons and mass ratio of negative (j) to positive (i) ions where $Q_\alpha = 1$ for $\alpha = i$ and $Q_\alpha = Q$ for $\alpha = j$.

In this paper, we are investigating only the fast mode large-amplitude compressive solitary waves and fast mode phase plane trajectories of bounded periodic solutions in two-temperature nonisothermal electron plasmas by the Sagdeev pseudo-potential method [9].

The normalized electron density (n_e) [31] for two-temperature nonisothermal electron plasma and the normalized positron density (n_p) are given in the following form:

$$n_e = n_{el} + n_{eh} =$$

$$= \mu\left[1 + \left(\frac{\phi}{\mu+\nu\beta_1}\right) - \frac{4}{3}b_l\left(\frac{\phi}{\mu+\nu\beta_1}\right)^{\frac{3}{2}} + \frac{1}{2}\left(\frac{\phi}{\mu+\nu\beta_1}\right)^2 - \right.$$

$$\left. - \frac{8}{15}b_l^{(1)}\left(\frac{\phi}{\mu+\nu\beta_1}\right)^{\frac{5}{2}} + \frac{1}{6}\left(\frac{\phi}{\mu+\nu\beta_1}\right)^3 + ...\right] +$$

$$+ \nu\left[1 + \left(\frac{\beta_1\phi}{\mu+\nu\beta_1}\right) - \frac{4}{3}b_h\left(\frac{\beta_1\phi}{\mu+\nu\beta_1}\right)^{\frac{3}{2}} + \frac{1}{2}\left(\frac{\beta_1\phi}{\mu+\nu\beta_1}\right)^2 - \right.$$

$$\left. - \frac{8}{15}b_h^{(1)}\left(\frac{\beta_1\phi}{\mu+\nu\beta_1}\right)^{\frac{5}{2}} + \frac{1}{6}\left(\frac{\beta_1\phi}{\mu+\nu\beta_1}\right)^3 + ...\right] =$$

$$= 1 + \phi - \frac{4}{3}\frac{\left(\mu b_l + \nu b_h \beta_1^{\frac{3}{2}}\right)}{(\mu+\nu\beta_1)^{\frac{3}{2}}}\phi^{\frac{3}{2}} + \frac{1}{2}\frac{(\mu+\nu\beta_1^2)}{(\mu+\nu\beta_1)^2}\phi^2 - $$

$$- \frac{8}{15}\frac{\left(\mu b_l^{(1)} + \nu b_h^{(1)}\beta_1^{\frac{5}{2}}\right)}{(\mu+\nu\beta_1)^{\frac{5}{2}}}\phi^{\frac{5}{2}} + \frac{1}{6}\frac{(\mu+\nu\beta_1^3)}{(\mu+\nu\beta_1)^3}\phi^3 - ..., \qquad (5)$$

$$n_p = \chi\, e^{-\sigma_p\phi}, \qquad (6)$$

where $\sigma_\alpha = \frac{T_\alpha}{T_{\text{eff}}}$, $\sigma_p = \frac{T_{\text{eff}}}{T_p}$, $Q_\alpha = \frac{m_\alpha}{m_i}$, $b_l = \frac{1-\beta_l}{\sqrt{\pi}}$, $b_h = \frac{1-\beta_h}{\sqrt{\pi}}$, $b_l^{(1)} = \frac{1-\beta_l^2}{\sqrt{\pi}}$, $b_h^{(1)} = \frac{1-\beta_h^2}{\sqrt{\pi}}$, $\beta_1 = \frac{T_{el,f}}{T_{eh,f}}$, $\beta_l = \frac{T_{el,f}}{T_{el,t}}$, $\beta_h = \frac{T_{eh,f}}{T_{eh,t}}$, $T_{\text{eff}} = \frac{T_{el}T_{eh}}{\mu T_{eh}+\nu T_{el}}$, $\mu+\nu = 1$.

Here, ϕ, x, t, T_α, T_p, σ_p are denoted respectively the electrostatic potential, space co-ordinate, time, the temperature of positive (negative) ions for $\boldsymbol{\alpha} = i$ and j, the temperature of positrons, temperature ratio of electrons and positrons with μ and ν are the unperturbed number density of low- and high-temperature electrons and $\boldsymbol{\chi}$ is the positron density at $\phi = 0$. Moreover, β_1, β_l and β_h are respectively the temperature ratio of free and trapped electrons in low- and high-temperatures; temperature ratio of free and trapped electrons in low temperature and temperature ratio of free and trapped electrons in high temperature.

For two-temperature nonisothermal plasma $0 < b_l$ or $b_h < \frac{1}{\sqrt{\pi}}$ and $0 < b_l^{(1)}$ or $b_h^{(1)} < \frac{1}{\sqrt{\pi}}$.

The physical quantities in the above equations are normalized in the following ways:

The densities n_α, n_e and n_p are normalized by their equilibrium values n_0 $[n_0 = n_{io} + n_{jo} = \mu + \nu = 1]$, ion pressures p_α by the characteristic ion pressure $p_0 = n_0 K_B T_\alpha$, the space co-ordinate x is normalized by the characteristic Debye length $\lambda_{De} = (K_B T_{eff}/4\pi e^2 n_{\alpha o})^{\frac{1}{2}}$, the time t by the plasma period $\omega_{p\alpha}^{-1} = (m_\alpha/4\pi e^2 n_{\alpha o})^{\frac{1}{2}}$ where K_B is Boltzmann' constant and e is the charge of an electrons, the ion velocities u_α by the ion sound velocity $C_S = (K_B T_{eff}/m_\alpha)^{\frac{1}{2}}$ where m_α is the mass of ions, and the electrostatic potential ϕ by $(K_B T_{eff}/e)$.

The boundary conditions for our plasma model are

$$n_\alpha \to n_{\alpha 0},\ u_\alpha \to u_{\alpha 0},\ p_\alpha \to 1,\ n_e \to 1,\ n_p \to \chi,$$
$$\phi \to 0 \text{ at } x \to \pm\infty \tag{7}$$

and the charge neutrality condition is

$$n_{p0} + \sum_\alpha Z_\alpha n_{\alpha 0} = 1. \tag{8}$$

Now, by the Galilean transformation, we transform the set of equations (1) to (4) to a frame moving with the wave through the co-moving co-ordinate $\eta = x - Vt$, where $V = (\frac{v}{C_S})$ denotes the speed of the nonlinear wave structures, normalized with respect to the ion sound velocity

$$-V\frac{\partial n_\alpha}{\partial \eta} + \frac{\partial}{\partial \eta}(n_\alpha u_\alpha) = 0, \tag{9}$$

$$-V\frac{\partial u_\alpha}{\partial \eta} + u_\alpha\frac{\partial u_\alpha}{\partial \eta} + \frac{\sigma_\alpha}{Q_\alpha n_\alpha}\frac{\partial p_\alpha}{\partial \eta} = -\frac{Z_\alpha}{Q_\alpha}\frac{\partial \phi}{\partial \eta}, \tag{10}$$

$$-V\frac{\partial p_\alpha}{\partial \eta} + u_\alpha\frac{\partial p_\alpha}{\partial \eta} + 3p_\alpha\frac{\partial u_\alpha}{\partial \eta} = 0, \tag{11}$$

$$\frac{\partial^2\phi}{\partial\eta^2} = n_e - \sum_\alpha Z_\alpha n_\alpha - n_p. \tag{12}$$

In equations (2) and (3) we have used the adiabatic pressure-density relation with poly tropic index $\gamma = 3$, that is $p_\alpha n_\alpha^{-3} = p_{\alpha 0}\,n_{\alpha 0}^{-3} = \text{const.}$

Since we consider the adiabatic case, Eqs. (2) and (3) for positive and negative ions, are consistent with the following equations of state in one-dimensional motion [32–33]

$$p_\alpha = p_{\alpha 0}\left(\frac{n_\alpha}{n_{\alpha 0}}\right)^3 \tag{13}$$

and, hence, we shall take $p_{\alpha 0} = 1$.

From the above equations after using the boundary conditions (8) and the equations of state, we get finally

$$n_\alpha = \sum_\alpha \sqrt{\frac{Q_\alpha n_{\alpha 0}^3}{12\sigma_\alpha}}\left[\left\{\left(V - u_{\alpha 0} + \sqrt{\frac{3\sigma_\alpha}{Q_\alpha n_{\alpha 0}}}\right)^2 - \frac{2Z_\alpha\phi}{Q_\alpha}\right\}^{\frac{1}{2}} \pm \left\{\left(V - u_{\alpha 0} - \sqrt{\frac{3\sigma_\alpha}{Q_\alpha n_{\alpha 0}}}\right)^2 - \frac{2Z_\alpha\phi}{Q_\alpha}\right\}^{\frac{1}{2}}\right]. \tag{14}$$

The choice of lower sign (minus) in the density expressions given by Eq. (14) are consistent with the boundary conditions (7). On substituting these in Poisson's equation in terms of η and integrating, it yields the energy integral-like equation

$$\frac{1}{2}\left(\frac{d\phi}{d\eta}\right)^2 + \psi(\phi) = 0, \tag{15}$$

where our expression for the Sagdeev pseudo-potential function reads as

$$\psi(\phi) = \left[-\phi - \frac{1}{2}\phi^2 + \frac{8}{15}\frac{\mu b_l + \nu b_h\beta_1^{\frac{3}{2}}}{(\mu + \nu\beta_1)^{\frac{3}{2}}}\phi^{\frac{5}{2}} - \frac{1}{6}\frac{\mu + \nu\beta_1^2}{(\mu + \nu\beta_1)^2}\phi^3 + \frac{16}{105}\frac{\mu b_l^{(1)} + \nu b_h^{(1)}\beta_1^{\frac{5}{2}}}{(\mu + \nu\beta_1)^{\frac{5}{2}}}\phi^{\frac{7}{2}} - \frac{1}{24}\frac{\mu + \nu\beta_1^3}{(\mu + \nu\beta_1)^3}\phi^4 + ...\right] + \sum_\alpha \frac{1}{6}\sqrt{\frac{Q_\alpha^3\,n_{\alpha 0}^3}{3\sigma_\alpha}}\left[\left\{\left(V - u_{\alpha 0} - \sqrt{\frac{3\sigma_\alpha}{Q_\alpha n_{\alpha 0}}}\right)^2 - \right.\right.$$

$$\ast \quad -\frac{2Z_\alpha\phi}{Q_\alpha}\Big\}^{\frac{3}{2}} - \Big\{\Big(V - u_{\alpha 0} + \sqrt{\frac{3\sigma_\alpha}{Q_\alpha n_{\alpha 0}}}\Big)^2 - \frac{2Z_\alpha\phi}{Q_\alpha}\Big\}^{\frac{3}{2}} +$$

$$+\Big(V - u_{\alpha 0} + \sqrt{\frac{3\sigma_\alpha}{Q_\alpha n_{\alpha 0}}}\Big)^3 - \Big(V - u_{\alpha 0} - \sqrt{\frac{3\sigma_\alpha}{Q_\alpha n_{\alpha 0}}}\Big)^3\Big] +$$

$$+\frac{\chi}{\sigma_p}(1 - e^{-\sigma_p\phi}). \tag{16}$$

The requirements to yield soliton solutions from the Sagdeev potential function $\psi(\phi)$ are

$\psi(\phi) = 0$ at $\phi = 0$ and $\phi = \phi_m$,

$\dfrac{\partial\psi}{\partial\phi} = 0$ at $\phi = 0$,

$\dfrac{\partial^2\psi}{\partial\phi^2} \leq 0$ at $\phi = 0$,

$\psi(\phi) < 0$ for $0 < \phi < \phi_m$ and $\phi > \phi_m$, $\tag{17}$

$\dfrac{\partial^3\psi}{\partial\phi^3} > 0$ at $\phi = 0$ for positive (compressive) potentials solitons,

$\dfrac{\partial\psi}{\partial\phi} > 0$ at $\phi = \phi_m$ for positive (compressive) potentials solitons.

For compressive solitons, the restriction on ϕ is obtained from the condition of the real values of the density of ions

$$0 < \phi < \frac{Q_\alpha}{2Z_\alpha}\Big(V - u_{\alpha 0} - \sqrt{\frac{3\sigma_\alpha}{Q_\alpha n_{\alpha 0}}}\Big)^2. \tag{18}$$

Therefore, the upper limit on the positive potential side is given by

$$\phi_l = \frac{1}{2}\Big(V - u_{i0} - \sqrt{\frac{3\sigma_i}{n_{i0}}}\Big)^2, \tag{19}$$

where ϕ_l is the limiting value of the potential for which the value of n_i remains positive and, beyond this, the value of n_i becomes negative. This implies that the amplitude ϕ_m cannot exceed the limiting value ϕ_l of the potential ϕ, which puts a limit on the maximum value of the phase velocity V. Putting $\phi = \phi_l$ in $\psi(\phi) = 0$, where streams of both ions are considered, we then get the maximum value of V.

The dispersion relation is found from condition (17) with equation (16) as

$$\sum_\alpha \frac{Z_\alpha^2 n_{\alpha 0}}{Q_\alpha(V - u_{\alpha 0})^2 - \frac{3\sigma_\alpha}{n_{\alpha 0}}} \leq 1 + \chi\sigma_p. \tag{20}$$

Equation (20) may be written in the following linear dispersion relation for positive (i) and negative (j) ions:

$$\frac{n_{i0}}{(V - u_{i0})^2 - \frac{3\alpha_i}{n_{i0}}} + \frac{Z^2 n_{j0}}{Q(V - u_{j0})^2 - \frac{3\alpha_j}{n_{j0}}} =$$

$$= 1 + \chi\sigma_p. \tag{21}$$

This is a nonlinear equation in V, where V is the phase velocity of the solitary waves. It is found that Eq. (21) in V has three distinct positive roots in which the smallest value of V is identified as a slow ion-acoustic mode (V_S), the intermediate root is a fast ion-acoustic mode (V_F), and the largest root is an electron-acoustic mode ($V_{e.acoust.}$). These critical values of V provide lower limits on the velocity ranges of solitons associated with the three different linear wave modes. When the temperatures of the positive (σ_i) and negative (σ_j) ions are the same ($\sigma_i = \sigma_j$), we get only the fast ion-acoustic mode. Maharaj *et al.* [27] showed that the critical Mach numbers for the fast ion-acoustic modes of solitons are lying between 2.3 and 4.5 in both inertial and Boltzmann hot electrons so that their phase speeds will lie between the hot ion and the cool electron thermal velocities. In this problem, we have the only interest on the phase velocity of fast mode (V_F), and we are trying to discuss the fast mode solitary waves related to this fast mode phase velocity (V_F). Experimental [34–37] and theoretical [38–41] studies have revealed that, in any two-ion species plasma with finite temperatures, the fast and slow wave modes propagate on the basis of the range of their following phase speeds with respect to the ion-thermal speeds:

$$v_{tc} < v_S < v_{th} < v_F < v_{tce} < v_{e.acoust.} < v_{the},$$

where v_{tc}, v_{th}, v_{tce} and v_{the} are the thermal speeds of colder ion species, hotter ion species, colder electrons and hotter electrons. In addition, v_S, v_F and $v_{e.acoust.}$ are respectively the phase speeds of the slow, fast, and the electron acoustic wave modes. For the further study, we take the following inequality for the fast and slow mode phase speeds in which the fast mode phase speed lies between the thermal speeds of hotter ion species and the colder electrons:

$$v_{tc} < v_S < v_{th} < v_F < v_{tce}.$$

The above inequality can be rewritten in the dimensionless form as

$$\sqrt{\frac{3\sigma_i}{n_{i0}}} < V_S < \sqrt{\frac{3\sigma_j}{Qn_{j0}}} < V_F < \frac{v_{tce}}{C_S},$$

where the normalization is done by the ion sound velocity C_S.

From Eq. (21), we are now discussing the different critical phase velocities (V_C) and its corresponding fast mode phase velocities (V_F) under some restrictions:

(i) **In general, when unequal streams ($u_{i0} \neq$ $\neq u_{j0}$, $u_{i0} \neq 0$, $u_{j0} \neq 0$) with warm positive (i) and warm negative (j) ions ($\sigma_i \neq 0$, $\sigma_j \neq 0$) are considered**, then equation (21) after simplifying some steps can be written in the following form:

$$V^4 - 2\left(u_{i0} + u_{j0}\right)V^3 + \left[\left\{\left(u_{j0}^2 + 4\,u_{i0}u_{j0} + u_{i0}^2\right) - \right.\right.$$
$$\left.- 3\left(\frac{\sigma_i}{n_{i0}} + \frac{\sigma_j}{Q\,n_{j0}}\right)\right\} - \frac{1}{(1 + \chi\,\sigma_p)}\left(n_{i0} + \frac{Z^2 n_{j0}}{Q}\right)\right]V^2 -$$
$$- 2\left[\left\{u_{i0}u_{j0}\left(u_{i0} + u_{j0}\right) - 3\left(\frac{u_{j0}\sigma_i}{n_{i0}} + \frac{u_{i0}\sigma_j}{Q\,n_{j0}}\right)\right\} + \right.$$
$$\left. + \frac{1}{(1 + \chi\,\sigma_p)}\left(n_{i0}u_{j0} + \frac{Z^2 n_{j0}u_{i0}}{Q}\right)\right]V +$$
$$+ \left[\left\{u_{i0}^2 u_{j0}^2 - 3\left(\frac{u_{j0}^2\sigma_i}{n_{i0}} + \frac{u_{i0}^2\sigma_j}{Q\,n_{j0}}\right) + \frac{9\sigma_i\sigma_j}{Qn_{i0}n_{j0}}\right\} - \right.$$
$$- \frac{1}{(1 + \chi\,\sigma_p)}\left\{n_{i0}u_{j0}^2 + \frac{Z^2 n_{j0}u_{i0}^2}{Q} - \right.$$
$$\left.\left. - \frac{3}{Q}\left(\frac{Z^2 n_{j0}\sigma_i}{n_{i0}} + \frac{n_{i0}\sigma_j}{n_{j0}}\right)\right\}\right] = 0. \tag{22}$$

This is a fourth-degree equation in V with most general form giving four real or imaginary values of the critical phase velocity V_c $(V = V_C)$, but we are only considering the real positive values of the fast mode phase velocity (V_F) which supports Ref. [42] and satisfies inequality (20) for $V = V_F > V_c$.

(ii) **For equal ion streams ($u_{i0} = u_{j0} = u_0$) when $\sigma_i \neq 0$, $\sigma_j \neq 0$**, then, writing $V -$ $- u_{i0} = V - u_{j0} = V_1$ (say), we get finally, from the equation (21)

$$\left(1 + \chi\,\sigma_p\right)V_1^4 - \left\{3\left(1 + \chi\,\sigma_p\right)\left(\frac{\sigma_i}{n_{i0}} + \frac{\sigma_j}{Q\,n_{j0}}\right) + \right.$$
$$\left. + \left(n_{i0} + \frac{Z^2 n_{j0}}{Q}\right)\right\}V_1^2 +$$
$$+ 3\left\{\frac{Z^2 n_{j0}\sigma_i}{Qn_{i0}} + \frac{n_{i0}\sigma_j}{Q\,n_{j0}} + 3\left(1 + \chi\,\sigma_p\right)\frac{\sigma_i\sigma_j}{Qn_{i0}n_{j0}}\right\} = 0.$$

This is a quadratic equation in V_1^2 which gives, after solving

$$V_1^2 = \frac{3}{2}\left[\left\{\left(\frac{\sigma_i}{n_{i0}} + \frac{\sigma_j}{Q\,n_{j0}}\right) + \frac{1}{3\left(1 + \chi\sigma_p\right)} \times \right.\right.$$
$$\times \left(n_{i0} + \frac{Z^2 n_{j0}}{Q}\right)\right\} \pm \left(\left\{\left(\frac{\sigma_i}{n_{i0}} + \frac{\sigma_j}{Q\,n_{j0}}\right) + \right.$$
$$+ \frac{1}{3\left(1 + \chi\sigma_p\right)}\left(n_{i0} + \frac{Z^2 n_{j0}}{Q}\right)\right\}^2 - \frac{4}{3}\left\{\frac{1}{(1 + \chi\sigma_p)} \times \right.$$
$$\left.\left.\times \left(\frac{Z^2 n_{j0}\sigma_i}{Qn_{i0}} + \frac{n_{i0}\sigma_j}{Q\,n_{j0}}\right) + \frac{3\sigma_i\sigma_j}{Qn_{i0}n_{j0}}\right\}\right)^{\frac{1}{2}}\right]. \tag{23}$$

The above expression gives two critical values of V_1^2 which are fully dependent on the ion temperatures σ_i and σ_j. Thus, we can say that the inclusion of a finite ion temperature gives rise to two ion-acoustic modes [21, 43–46] namely critical slow ion-acoustic wave mode $(V_1)_{CS}$ and critical fast ion-acoustic wave mode $(V_1)_{CF}$ propagating with the different phase velocities when equal ion streams (u_0) are taken. For the further study, we will consider only the fast wave mode.

The critical values of the phase velocity of fast ion-acoustic wave mode is

$$(V_1)_{CF}^2 = \frac{3}{2}\left[\left\{\left(\frac{\sigma_i}{n_{i0}} + \frac{\sigma_j}{Q\,n_{j0}}\right) + \frac{1}{3\left(1 + \chi\sigma_p\right)} \times \right.\right.$$
$$\times \left(n_{i0} + \frac{Z^2 n_{j0}}{Q}\right)\right\} + \left(\left\{\left(\frac{\sigma_i}{n_{i0}} + \frac{\sigma_j}{Q\,n_{j0}}\right) + \right.$$
$$+ \frac{1}{3\left(1 + \chi\sigma_p\right)}\left(n_{i0} + \frac{Z^2 n_{j0}}{Q}\right)\right\}^2 - \frac{4}{3}\left\{\frac{1}{(1 + \chi\sigma_p)} \times \right.$$
$$\left.\left.\times \left(\frac{Z^2 n_{j0}\sigma_i}{Qn_{i0}} + \frac{n_{i0}\sigma_j}{Q\,n_{j0}}\right) + \frac{3\sigma_i\sigma_j}{Qn_{i0}n_{j0}}\right\}\right)^{\frac{1}{2}}\right]. \tag{24}$$

Thus, the modified fast ion-acoustic critical phase velocity (V_{MCF}) is

$$V_{MCF} = u_0 + (V_1)_{CF},$$
$$V_{MCF} = u_0 + \left\{\frac{3}{2}\left[\left\{\left(\frac{\sigma_i}{n_{i0}} + \frac{\sigma_j}{Q\,n_{j0}}\right) + \frac{1}{3\left(1 + \chi\sigma_p\right)} \times \right.\right.\right.$$
$$\times \left(n_{i0} + \frac{Z^2 n_{j0}}{Q}\right)\right\} + \left(\left\{\left(\frac{\sigma_i}{n_{i0}} + \frac{\sigma_j}{Q\,n_{j0}}\right) + \frac{1}{3\left(1 + \chi\sigma_p\right)} \times \right.\right.$$
$$\times \left(n_{i0} + \frac{Z^2 n_{j0}}{Q}\right)\right\}^2 - \frac{4}{3}\left\{\frac{1}{(1 + \chi\sigma_p)} \times \right.$$
$$\left.\left.\left.\times \left(\frac{Z^2 n_{j0}\sigma_i}{Qn_{i0}} + \frac{n_{i0}\sigma_j}{Q\,n_{j0}}\right) + \frac{3\sigma_i\sigma_j}{Qn_{i0}n_{j0}}\right\}\right)^{\frac{1}{2}}\right]\right\}^{\frac{1}{2}}. \tag{25}$$

Now, from Eq. (23) by Taylor series expansion to the zeroth order, we get approximately as

$$V_1^2 = (V - u_0)^2 \approx \frac{3\sigma_j}{Q\,n_{j0}} + \frac{3\sigma_i}{n_{i0}} +$$
$$+ \frac{n_{i0}}{(1 + \chi\sigma_p)} + \frac{Z^2 n_{j0}}{Q\,(1 + \chi\sigma_p)}, \tag{26}$$

which shows
$$V_1^2 = (V - u_0)^2 > \frac{3\sigma_j}{Q\,n_{j0}} \Rightarrow$$

$$\Rightarrow V_1 = (V - u_0) > \sqrt{\frac{3\sigma_j}{Q\,n_{j0}}} \Rightarrow$$

$$\Rightarrow V > u_0 + \sqrt{\frac{3\sigma_j}{Q\,n_{j0}}}. \tag{27}$$

This means that the fast mode phase velocity is greater than the value of $\sqrt{\frac{3\sigma_j}{Q\,n_{j0}}}$.

(iii) **When equal ion temperatures ($\sigma_i = \sigma_j = \sigma$) and equal ion streams ($u_{i0} = u_{j0} = u_0$) are taken**. Then we get, from Eq. (21),

$$\frac{n_{i0}}{(V - u_0)^2 - \frac{3\sigma}{n_{i0}}} + \frac{Z^2 n_{j0}}{Q\,(V - u_0)^2 - \frac{3\sigma}{n_{j0}}} = 1 + \chi\sigma_p.$$

After a simplification, we get

$$V_1^2 = \frac{3}{2}\Bigg[\bigg\{\sigma\left(\frac{1}{n_{i0}} + \frac{1}{Q\,n_{j0}}\right) + \frac{1}{3\,(1 + \chi\sigma_p)} \times$$
$$\times \left(n_{i0} + \frac{Z^2 n_{j0}}{Q}\right)\bigg\} \pm \bigg(\bigg\{\sigma\left(\frac{1}{n_{i0}} + \frac{1}{Q\,n_{j0}}\right) +$$
$$+ \frac{1}{3\,(1 + \chi\sigma_p)}\left(n_{i0} + \frac{Z^2 n_{j0}}{Q}\right)\bigg\}^2 - \frac{4\sigma}{3Q}\bigg\{\frac{1}{(1 + \chi\sigma_p)} \times$$
$$\times \left(\frac{Z^2 n_{j0}}{n_{i0}} + \frac{n_{i0}}{n_{j0}}\right) + \frac{3\sigma}{n_{i0}n_{j0}}\bigg\}\bigg)^{\frac{1}{2}}\Bigg],$$

where $V_1 = (V - u_{i0}) = (V - u_{j0}) = (V - u_o)$.

Taking positive sign (+), the fast mode critical phase velocity $\left[(V_1)_{CF}^2\right]$ is

$$(V_1)_{CF}^2 = \frac{3}{2}\Bigg[\bigg\{\sigma\left(\frac{1}{n_{i0}} + \frac{1}{Q\,n_{j0}}\right) + \frac{1}{3\,(1 + \chi\sigma_p)} \times$$
$$\times \left(n_{i0} + \frac{Z^2 n_{j0}}{Q}\right)\bigg\} + \bigg(\bigg\{\sigma\left(\frac{1}{n_{i0}} + \frac{1}{Q\,n_{j0}}\right) +$$

$$+ \frac{1}{3\,(1 + \chi\sigma_p)}\left(n_{i0} + \frac{Z^2 n_{j0}}{Q}\right)\bigg\}^2 - \frac{4\sigma}{3Q}\bigg\{\frac{1}{(1 + \chi\sigma_p)} \times$$
$$\times \left(\frac{Z^2 n_{j0}}{n_{i0}} + \frac{n_{i0}}{n_{j0}}\right) + \frac{3\sigma}{n_{i0}n_{j0}}\bigg\}\bigg)^{\frac{1}{2}}\Bigg]. \tag{28}$$

Thus,

$$V_{CF} = u_0 + (V_1)_{CF} =$$
$$= u_0 + \Bigg\{\frac{3}{2}\bigg[\bigg\{\sigma\left(\frac{1}{n_{i0}} + \frac{1}{Q\,n_{j0}}\right) + \frac{1}{3\,(1 + \chi\sigma_p)} \times$$
$$\times \left(n_{i0} + \frac{Z^2 n_{j0}}{Q}\right)\bigg\} + \bigg(\bigg\{\sigma\left(\frac{1}{n_{i0}} + \frac{1}{Q\,n_{j0}}\right) +$$
$$+ \frac{1}{3\,(1 + \chi\sigma_p)}\left(n_{i0} + \frac{Z^2 n_{j0}}{Q}\right)\bigg\}^2 - \frac{4\sigma}{3Q}\bigg\{\frac{1}{(1 + \chi\sigma_p)} \times$$
$$\times \left(\frac{Z^2 n_{j0}}{n_{i0}} + \frac{n_{i0}}{n_{j0}}\right) + \frac{3\sigma}{n_{i0}n_{j0}}\bigg\}\bigg)^{\frac{1}{2}}\bigg]\Bigg\}^{\frac{1}{2}}. \tag{29}$$

The above value of the critical phase velocity for the fast mode (V_{CF}) depends on the stream velocity and ion temperatures. It is remarkable to mention that V_{CF} is meaningful even if $u_o = 0$.

(iv) **When unequal streams ($u_{i0} \neq u_{j0}$, $u_{i0} = 0$, $u_{j0} \neq 0$) with warm positive (σ_i) and warm negative (σ_j) ions ($\sigma_i \neq 0$, $\sigma_j \neq 0$) are considered**, then Eq. (21) reduces to the form

$$\frac{n_{i0}}{V^2 - \frac{3\sigma}{n_{i0}}} + \frac{Z^2 n_{j0}}{Q\,(V - u_{j0})^2 - \frac{3\sigma}{n_{j0}}} = 1 + \chi\sigma_p.$$

After simplifying some steps, we can write the above equation in the following form:

$$V^4 - 2u_{j0}V^3 + \Bigg[\bigg\{u_{j0}^2 - 3\left(\frac{\sigma_i}{n_{i0}} + \frac{\sigma_j}{Q\,n_{j0}}\right)\bigg\} -$$
$$- \frac{1}{(1 + \chi\,\sigma_p)}\left(n_{i0} + \frac{Z^2 n_{j0}}{Q}\right)\Bigg]V^2 -$$
$$- 2\left[\frac{n_{i0}u_{j0}}{(1 + \chi\,\sigma_p)} - \frac{3\sigma_i u_{j0}}{n_{i0}}\right]V +$$
$$+ \Bigg[\bigg\{\frac{9\sigma_i\sigma_j}{Q n_{i0}n_{j0}} - \frac{3\sigma_i u_{j0}^2}{n_{i0}}\bigg\} - \frac{1}{(1 + \chi\,\sigma_p)}\bigg\{n_{i0}u_{j0}^2 -$$
$$- \frac{3}{Q}\left(\frac{Z^2 n_{j0}\sigma_i}{n_{i0}} + \frac{n_{i0}\sigma_j}{n_{j0}}\right)\bigg\}\Bigg] = 0. \tag{30}$$

This is, a biquadratic equation in V giving four real or imaginary values of the critical phase velocity ($V = V_C$), but we are only considering the real positive values of the fast mode phase velocity ($V_F > V_C$) which supports Ref. [31] and satisfies inequality (20).

3. Fast Mode Phase Plane Trajectories

In a two-temperature electron plasma, the fast mode will generally involve compressional oscillations of the plasma which affects both the ion and electron densities. The nonisothermal nature means that the temperatures of the electron species and ion species differ, which can result in different propagation speeds and wave modes depending on the densities and temperatures of each species.

The phase plane trajectories in this scenario is a tool to visualize the evolution of the plasma state in time. It typically involves plotting two quantities that describe the plasma's state at any given moment, such as the density perturbation of the plasma and the velocity perturbation for each species.

For the fast mode wave in an unmagnetized two-temperature plasma, the phase plane would illustrate how these perturbations evolve, when the wave propagates. The fast mode phase plane trajectories could describe the behaviour of the plasma's density and velocity fluctuations, as the wave moves through the plasma, with regard for the different responses of the multiple species (electrons, ions, and positrons) with their distinct temperatures.

The fast mode phase plane trajectory specifically describes the path that the fast-changing variables follow within the phase plane, while the slow-changing variables are either approximated as constants or evolve more gradually. In practice, when examining such a system, we might first "reduce" the system by focussing on the fast variables to understand how they behave themselves and later consider how the slow variables influence the dynamics.

From energy integral-like equation (10), we can write

$$\frac{1}{2}\left(\frac{d\phi}{d\eta}\right)^2 + \psi(\phi) = 0 \Rightarrow$$

$$\Rightarrow \frac{d\phi}{d\eta} = \pm\sqrt{-2\psi(\phi)}, \tag{31}$$

where $\psi(\phi)$ is the Sagdeev potential function, and ϕ is the electrostatic potential. The diagrams for plotting of $\frac{d\phi}{d\eta}$ against ϕ represents the phase plane trajectories which are symmetric about the ϕ axis and is known as the bounded periodic solutions of the fast mode solitary waves.

The fast mode phase plane trajectories in a multi-species, unmagnetized, nonisothermal plasma system

provide a detailed understanding of the collective dynamics of the plasma. These trajectories are used to model and analyze wave propagation, instabilities, energy transfer and interactions between different species, with important applications in fusion research, space physics, diagnostics and plasma electronics. The analysis of these trajectories enables a better prediction and control over the plasma behavior in both laboratory and astrophysical environments.

4. Results and Discussions

In this section, we are comprehensively discussing the large-amplitude ion-acoustic fast mode compressive solitons and the fast mode phase plane trajectories of the bounded periodic solutions under the variation of the streaming motion of positive (u_{i0}) and negative (u_{j0}) ions, the different values of V, the temperatures of both positive (σ_i) and negative (σ_j) ions and the concentrations of negative ions (n_{j0}). These are shown in Figs. 1 to 8. In this paper, for our chosen set of arbitrary plasma parameters, it is found that the fast mode phase velocity V_F $(V = V_F)$ satisfying inequality (14), is generally greater than the critical phase velocity V_c for the formation of the large-amplitude ion-acoustic fast mode solitons and fast mode phase plane trajectories.

In Fig. 1, *a*, the Sagdeev potential function $\psi(\phi)$ against ϕ for large-amplitude ion-acoustic fast mode compressive solitons are shown under the variation of the streaming motion of positive (u_{i0}) and negative (u_{j0}) ions for $n_{j0} = 0.05$, $n_{i0} = 0.88$, $\sigma_i = \frac{1}{30}$, $\sigma_j = \frac{1}{20}$, $\chi = 0.17$, $V = 1.55$, $\sigma_p = 0.41$, $Z = 1$, $\beta_1 = 0.25$, $\mu = 0.15$, $\nu = 0.85$, $b_l = 0.15$, $b_h = 0.4$, $b_l^{(1)} = 0.24$, $b_h^{(1)} = 0.51$, when $fu_{i0} = 0.4$, $u_{j0} = 0.2$; $u_{i0} = 0.44$, $u_{j0} = 0.24$; $u_{i0} = 0.46$, $u_{j0} = 0.26$; $u_{i0} = 0.48$, $u_{j0} = 0.28$ are denoted, respectively, by the curves a_1, a_2, a_3, and a_4. The curves a_1, a_2, and a_3 show the exact solitonic nature, but a_4 does not show such nature. It is found further that the amplitudes of these curves are increasing, when the streams of the positive and negative ions are decreasing and the depth of the well is also decreasing.

Figure 1, *b* shows the Sagdeev potential function $\psi(\phi)$ against ϕ for the large-amplitude ion-acoustic fast mode compressive solitons under the variation of the streaming motion of positive (u_{i0}) and negative (u_{j0}) ions for $n_{j0} = 0.03$, $n_{i0} = 0.86$, $\sigma_i = \frac{1}{100}$, $\sigma_j = \frac{1}{20}$, $\chi = 0.17$, $V = 1.6$, $\sigma_p = 0.41$, $Z = 1$,
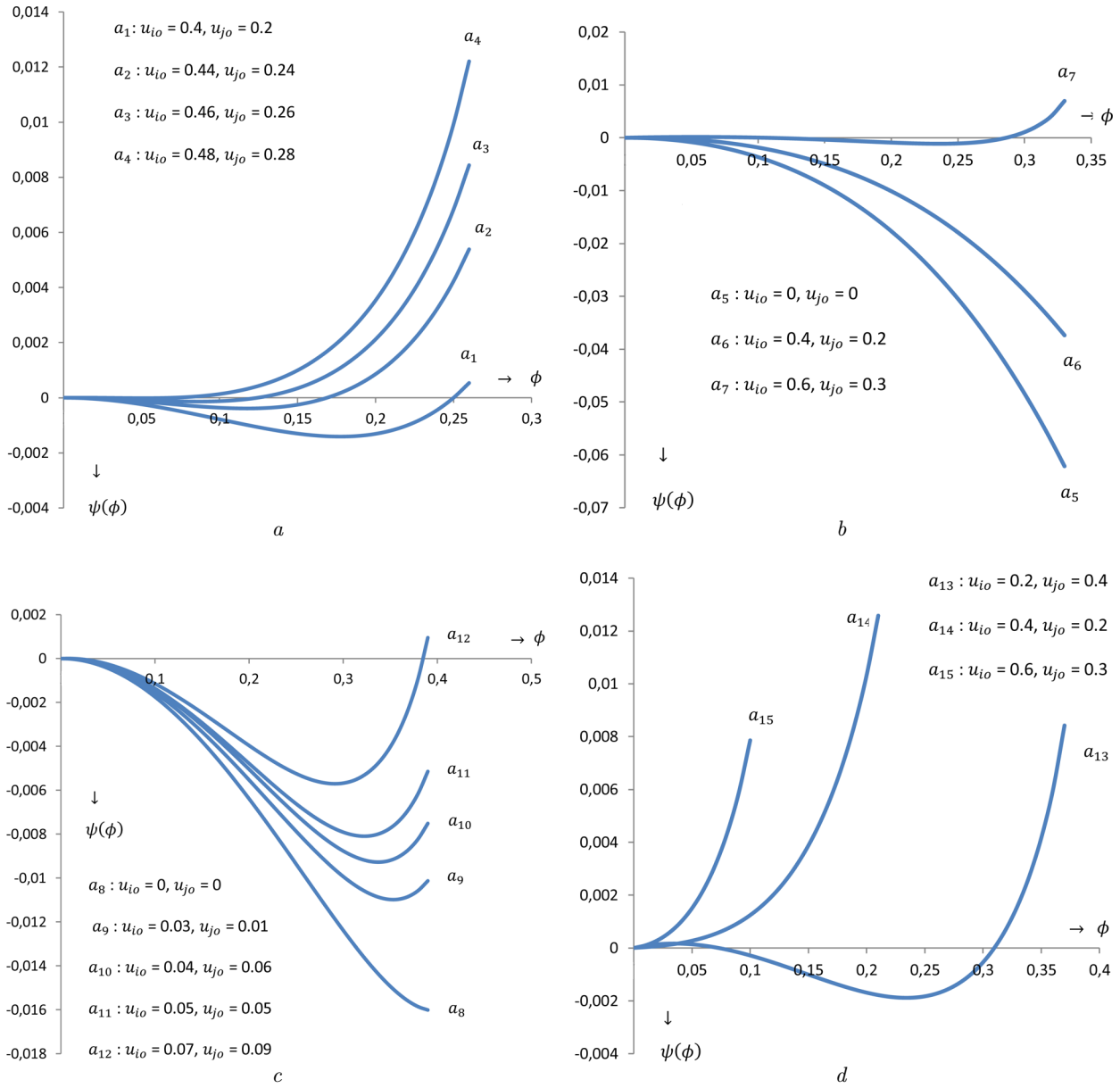
Fig. 1. The Sagdeev potential profiles $\psi(\phi)$ against ϕ for the large-amplitude ion-acoustic fast mode compressive solitons in two-temperature nonisothermal electron plasmas under the variation of the stream velocities of positive (u_{i0}) and negative (u_{j0}) ions for: $a - n_{j0} = 0.05$, $n_{i0} = 0.88$, $\sigma_i = \frac{1}{30}$, $\sigma_j = \frac{1}{20}$, $\chi = 0.17$, $V = 1.55$, $\sigma_p = 0.41$, $Z = 1$, $\beta_1 = 0.25$, $\mu = 0.15$, $\nu = 0.85$, $b_l = 0.15$, $b_h = 0.4$, $b_l^{(1)} = 0.24$, $b_h^{(1)} = 0.51$, when $u_{i0} = 0.4$, $u_{j0} = 0.2$, $u_{i0} = 0.44$, $u_{j0} = 0.24$; $u_{i0} = 0.46$, $u_{j0} = 0.26$; $u_{i0} = 0.48$, $u_{j0} = 0.28$; $b - n_{j0} = 0.03$, $n_{i0} = 0.86$, $\sigma_i = \frac{1}{100}$, $\sigma_j = \frac{1}{20}$ $\chi = 0.17$, $V = 1.6$, $\sigma_p = 0.41$, $Z = 1$, $\beta_1 = 0.02$, $\mu = 0.15$, $\nu = 0.85$, $b_l = 0.15$, $b_h = 0.4$, $b_l^{(1)} = 0.24$, $b_h^{(1)} = 0.51$ when $u_{i0} = 0$, $u_{j0} = 0$, $u_{i0} = 0.4$, $u_{j0} = 0.2$, $u_{i0} = 0.6$, $u_{j0} = 0.3$; $c - n_{j0} = 0.05$, $n_{i0} = 0.88$, $\sigma_i = \frac{1}{30}$, $\sigma_j = \frac{1}{20}$, $\chi = 0.17$, $V = 1.3$, $\sigma_p = 0.41$, $Z = 1$, $\beta_1 = 0.25$, $\mu = 0.15$, $\nu = 0.85$, $b_l = 0.15$, $b_h = 0.4$, $b_l^{(1)} = 0.24$, $b_h^{(1)} = 0.51$, when $u_{i0} = 0$, $u_{j0} = 0$; $u_{i0} = 0.03$, $u_{j0} = 0.01$, $u_{i0} = 0.04$, $u_{j0} = 0.06$; $u_{i0} = 0.05$, $u_{j0} = 0.05$, $u_{i0} = 0.07$, $u_{j0} = 0.09$; $d - n_{j0} = 0.05$, $n_{i0} = 0.88$, $\sigma_i = \frac{1}{30}$, $\sigma_j = \frac{1}{20}$, $\chi = 0.17$, $V = 1.4$, $\sigma_p = 0.41$, $Z = 1$, $\beta_1 = 0.25$, $\mu = 0.15$, $\nu = 0.85$, $b_l = 0.15$, $b_h = 0.4$, $b_l^{(1)} = 0.24$, $b_h^{(1)} = 0.51$, when $u_{i0} = 0$, $u_{j0} = 0.4$, $u_{i0}0.4$, $u_{j0} = 0.2$, $u_{i0} = 0.6$, $u_{j0} = 0.3$
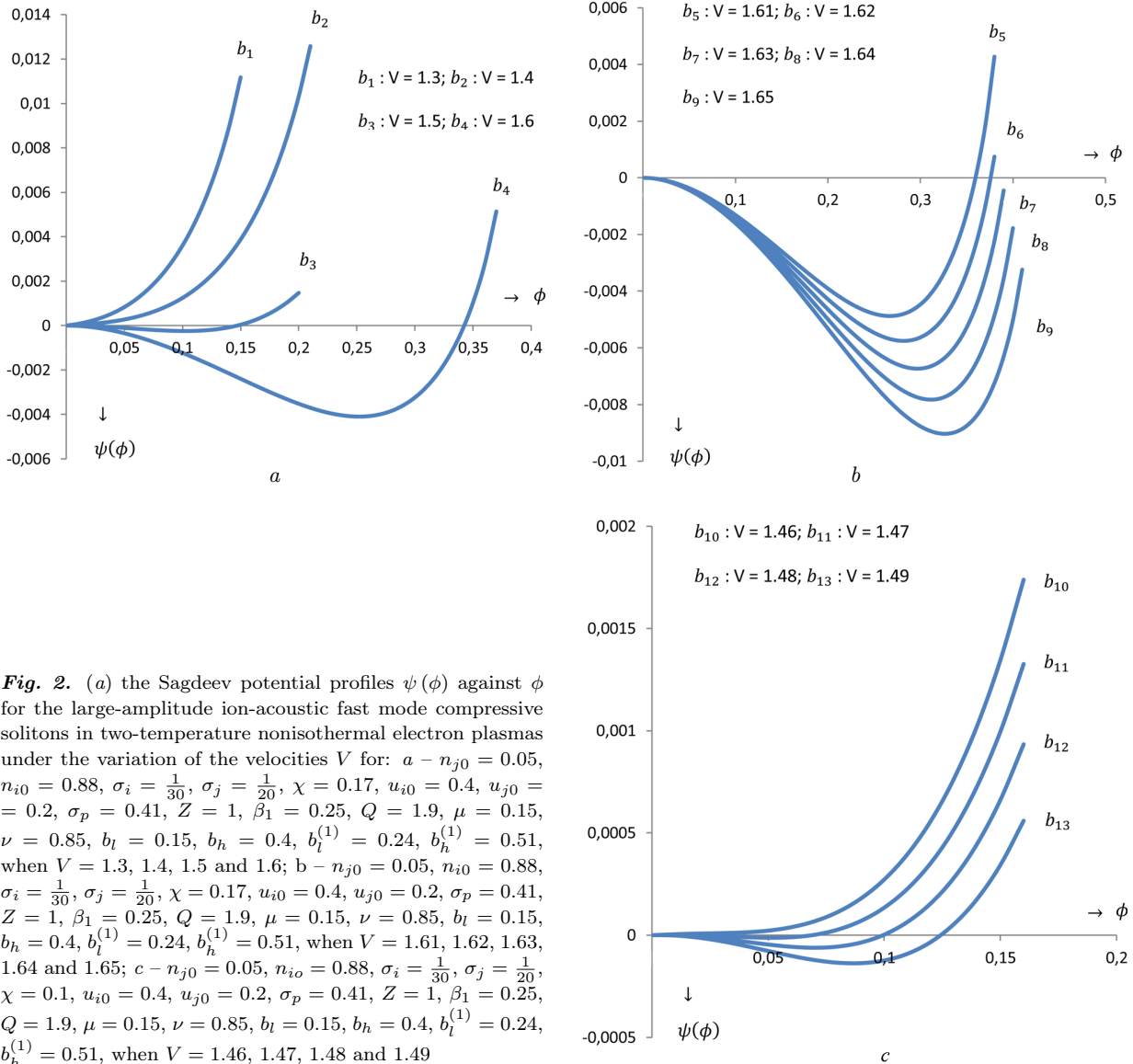
Fig. 2. (*a*) the Sagdeev potential profiles $\psi(\phi)$ against ϕ for the large-amplitude ion-acoustic fast mode compressive solitons in two-temperature nonisothermal electron plasmas under the variation of the velocities V for: $a - n_{j0} = 0.05$, $n_{i0} = 0.88$, $\sigma_i = \frac{1}{30}$, $\sigma_j = \frac{1}{20}$, $\chi = 0.17$, $u_{i0} = 0.4$, $u_{j0} = 0.2$, $\sigma_p = 0.41$, $Z = 1$, $\beta_1 = 0.25$, $Q = 1.9$, $\mu = 0.15$, $\nu = 0.85$, $b_l = 0.15$, $b_h = 0.4$, $b_l^{(1)} = 0.24$, $b_h^{(1)} = 0.51$, when $V = 1.3$, 1.4, 1.5 and 1.6; b $- n_{j0} = 0.05$, $n_{i0} = 0.88$, $\sigma_i = \frac{1}{30}$, $\sigma_j = \frac{1}{20}$, $\chi = 0.17$, $u_{i0} = 0.4$, $u_{j0} = 0.2$, $\sigma_p = 0.41$, $Z = 1$, $\beta_1 = 0.25$, $Q = 1.9$, $\mu = 0.15$, $\nu = 0.85$, $b_l = 0.15$, $b_h = 0.4$, $b_l^{(1)} = 0.24$, $b_h^{(1)} = 0.51$, when $V = 1.61$, 1.62, 1.63, 1.64 and 1.65; $c - n_{j0} = 0.05$, $n_{io} = 0.88$, $\sigma_i = \frac{1}{30}$, $\sigma_j = \frac{1}{20}$, $\chi = 0.1$, $u_{i0} = 0.4$, $u_{j0} = 0.2$, $\sigma_p = 0.41$, $Z = 1$, $\beta_1 = 0.25$, $Q = 1.9$, $\mu = 0.15$, $\nu = 0.85$, $b_l = 0.15$, $b_h = 0.4$, $b_l^{(1)} = 0.24$, $b_h^{(1)} = 0.51$, when $V = 1.46$, 1.47, 1.48 and 1.49

$\beta_1 = 0.02$, $\mu = 0.15$, $\nu = 0.85$, $b_l = 0.15$, $b_h = 0.4$, $b_l^{(1)} = 0.24$, $b_h^{(1)} = 0.51$, when $u_{i0} = 0$, $u_{j0} = 0$; $u_{i0} = 0.4$, $u_{j0} = 0.2$; $u_{i0} = 0.6$, $u_{j0} = 0.3$ represented by the curves a_5, a_6, and a_7, respectively. These curves do not show any exact solitonic nature for our used plasma parameters.

In Fig. 1, c, the Sagdeev potential function $\psi(\phi)$ against ϕ for the large-amplitude ion-acoustic fast mode compressive solitons are shown under the variation of the streaming motion of positive (u_{io}) and negative (u_{j0}) ions for $n_{j0} = 0.05$, $n_{i0} = 0.88$, $\sigma_i = \frac{1}{30}$,

$\sigma_j = \frac{1}{20}$, $\chi = 0.17$, $V = 1.3$, $\sigma_p = 0.41$, $Z = 1$, $\beta_1 = 0.25$, $\mu = 0.15$, $\nu = 0.85$, $b_l = 0.15$, $b_h = 0.4$, $b_l^{(1)} = 0.24$, $b_h^{(1)} = 0.51$, when $u_{i0} = 0$, $u_{j0} = 0$; $u_{i0} = 0.03$, $u_{j0}0.01$; $u_{i0} = 0.04$, $u_{j0} = 0.06$; $u_{i0} = 0.05$, $u_{j0} = 0.05$; $u_{i0} = 0.07$, $u_{j0} = 0.09$ denoted respectively by the curves a_8, a_9, a_{10}, a_{11}, and a_{12}. But only the curve a_{12} shows the solitonic nature for $u_{i0} = 0.07$, $u_{j0} = 0.09$ with $V = 1.3$, $n_{j0} = 0.05$ and $\sigma_i = \frac{1}{30}$, $\sigma_j = \frac{1}{20}$ which is an exceptional case due to the high stream velocities of positive and negative ions.

Figure 1, *d* shows the Sagdeev potential function $\psi(\phi)$ against ϕ for the large-amplitude ion-acoustic fast mode compressive solitons under the variation of the streaming motion of positive (u_{i0}) and negative (u_{j0}) ions for $n_{j0} = 0.05$, $n_{i0} = 0.88$, $\sigma_i = \frac{1}{30}$, $\sigma_j = \frac{1}{20}$, $\chi = 0.17$, $V = 1.4$, $\sigma_p = 0.41$, $Z = 1$, $\beta_1 = 0.25$, $\mu = 0.15$, $\nu = 0.85$, $b_l = 0.15$, $b_h = 0.4$, $b_l^{(1)} = 0.24$, $b_h^{(1)} = 0.51$ when $u_{i0} = 0.2$, $u_{j0} = 0.4$; $u_{i0} = 0.4$, $u_{j0} = 0.2$; $u_{i0} = 0.6$, $u_{j0} = 0.3$ represented by the curves a_{13}, a_{14}, and a_{15}, respectively. These curves do not show any exact solitonic nature for our used plasma parameters in this model.

The streaming motions of positive and negative ions affect the nonlinearity and dispersion of the plasma waves. Specifically, the relative streaming velocities between these ion species alter the balance between nonlinearity and dispersion which is crucial in soliton formation. An increase in the relative streaming velocity generally leads to an increase in soliton amplitude and a decrease in soliton width and, this is due to enhanced nonlinearity resulting from stronger interaction among the species. Actually streaming motions generally modify the effective Mach number for the fast mode solitons, altering their propagation speed, and enhances the nonisothermal effects. This effect is linked to the combined influence of ion inertia and the pressure of the warm positive and negative ions.

In Fig. 2, *a*, the Sagdeev potential function $\psi(\phi)$ against ϕ for the large-amplitude ion-acoustic fast mode compressive solitons are shown under the variation of the different values of V for $n_{j0} = 0.05$, $n_{i0} = 0.88$, $\sigma_i = \frac{1}{30}$, $\sigma_j = \frac{1}{20}$, $\chi = 0.17$, $u_{i0} = 0.4$, $u_{j0} = 0.2$; $\sigma_p = 0.41$, $Z = 1$, $\beta_1 = 0.25$, $\mu = 0.15$, $\nu = 0.85$, $b_l = 0.15$, $b_h = 0.4$, $b_l^{(1)} = 0.24$, $b_h^{(1)} = 0.51$ when $V = 1.3$, 1.4, 1.5, 1.6 denoted respectively by the curves b_1, b_2, b_3, and b_4. Out of these four curves, only b_3 and b_4 show the exact solitonic nature, while the other two b_1 and b_2 do not show such nature for our used plasma parameters.

Figure 2, *b* shows the Sagdeev potential function $\psi(\phi)$ against ϕ for the large-amplitude ion-acoustic fast mode compressive solitons under the variation of the different values of V for $n_{j0} = 0.05$, $n_{i0} = 0.88$, $\sigma_i = \frac{1}{30}$, $\sigma_j = \frac{1}{20}$, $\chi = 0.17$, $u_{i0} = 0.4$, $u_{j0} = 0.2$; $\sigma_p = 0.41$, $Z = 1$, $\beta_1 = 0.25$, $\mu = 0.15$, $\nu = 0.850$ $b_l = 0.15$, $b_h = 0.4$, $b_l^{(1)} = 0.24$, $b_h^{(1)} = 0.51$, when $V = 1.61$, 1.62, 1.63, 1.64, 1.65 represented by the

curves b_5, b_6, b_7, b_8, and b_9, respectively. The curves b_5 for $V = 1.61$ and b_6 for $V = 1.62$ show the exact solitonic nature, while the others b_7, b_8, and b_9 for $V = 1.63$, 1.64 and 1.65 do not show such nature for our used plasma parameters.

In Fig. 2, *c*, the Sagdeev potential function $\psi(\phi)$ against ϕ for the large-amplitude ion-acoustic fast mode compressive solitons are shown under the variation of the different values of V for $n_{j0} = 0.05$, $n_{i0} = 0.88$, $\sigma_i = \frac{1}{30}$, $\sigma_j = \frac{1}{20}$, $\chi = 0.17$, $u_{i0} = 0.4$, $u_{j0} = 0.2$; $\sigma_p = 0.41$, $Z = 1$, $\beta_1 = 0.25$, $\mu = 0.15$, $\nu = 0.85$, $b_l = 0.15$, $b_h = 0.4$, $b_l^{(1)} = 0.24$, $b_h^{(1)} = 0.51$, when $V = 1.46$, 1.47, 1.48, 1.49 denoted respectively by the curves b_{10}, b_{11}, b_{12}, and b_{13}. The Sagdeev potential curves b_{12} for $V = 1.48$ and b_{13} for $V = 1.49$ represent the exact solitonic nature, but the other two b_{10} and b_{11} for $V = 1.46$ and 1.47 do not show any solitonic behavior for our model plasma.

The amplitude and width of the fast mode solitons are directly affected by the phase velocity. The phase velocity determines the range of parameters for which the stable fast mode solitons can exist. Consequently, the phase velocity affects the nonlinearity through its impact on the ion densities and pressures. Since the plasma is nonisothermal, the thermal speeds of ions and positrons contribute to the dispersive properties, influencing the soliton profile.

In our model plasma, the phase velocity V ($V = V_F$) must lies within a specific interval $1.48 \leq V \leq 1.62$ for the fast mode compressive solitons to exist. It is typically related to the fast mode speed, which is influenced by the combined thermal pressures and inertial effects of all species. If it is too low or too high relative to the characteristic sound speeds of the plasma components, the balance between nonlinearity and dispersion required for soliton formation is disrupted, preventing soliton propagation. It is further mentioned that the solitonic nature is also found even if $V = V_F = 1.3$ for $n_{j0} = 0.05$, $n_{i0} = 0.88$, $\sigma_i = \frac{1}{30}$, $\sigma_j = \frac{1}{20}$, $\chi = 0.17$, $\sigma_p = 0.41$, $Z = 1$, $\beta_1 = 0.25$, $\mu = 0.15$, $\nu = 0.85$, $b_l = 0.15$, $b_h = 0.4$, $b_l^{(1)} = 0.24$, $b_h^{(1)} = 0.51$, when $u_{i0} = 0.07$, $u_{j0} = 0.09$ and this possible due to high stream velocities of positive and negative ions. Higher phase velocities generally lead to larger or increasing amplitude and narrower or decreasing width of the solitons. Conversely, lower phase velocities yield smaller amplitude and broader solitons due to a weaker nonlinear steepening effect. The phase velocity plays a crucial role in
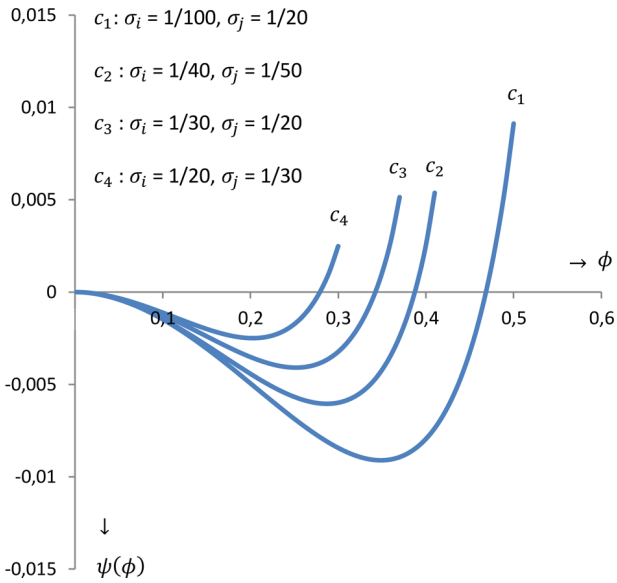
Fig. 3. Sagdeev potential profiles $\psi(\phi)$ against ϕ for large amplitude ion-acoustic fast mode compressive solitons in two-temperature nonisothermal electron plasmas under the variation of the temperatures of positive (σ_i) and negative (σ_j) ions for $n_{j0} = 0.05$, $n_{i0} = 0.88$, $\chi = 0.17$, $V = 0.17, 1.6$, $u_{i0} = 0.4$, $u_{j0} = 0.2$, $\sigma_p = 0.41$, $Z = 1$, $\beta_1 = 0.25$, $Q = 1.9$, $\mu = 0.15$, $\nu = 0.85$, $b_l = 0.15$, $b_h = 0.4$, $b_l^{(1)} = 0.24$, $b_h^{(1)} = 0.51$ when $\sigma_i = \frac{1}{100}$, $\sigma_j = \frac{1}{20}$; $\sigma_i = \frac{1}{40}$, $\sigma_j = \frac{1}{50}$; $\sigma_i = \frac{1}{30}$, $\sigma_j = \frac{1}{20}$; $\sigma_i = \frac{1}{20}$, $\sigma_j = \frac{1}{30}$

Fig. 4. Sagdeev potential profiles $\psi(\phi)$ against ϕ for the large-amplitude ion-acoustic fast mode compressive solitons in two-temperature nonisothermal electron plasmas under the variation of the concentrations of negative (n_{j0}) ions for $\sigma_i = \frac{1}{30}$, $\sigma_j = \frac{1}{20}$; $\chi = 0.17$, $V = 1.6$, $u_{i0} = 0.4$, $u_{j0} = 0.2$, $\sigma_p = 0.41$, $Z = 1$, $\beta_1 = 0.25$, $Q = 1.9$, $\mu = 0.15$, $\nu = 0.85$, $b_l = 0.15$, $b_h = 0.4$, $b_l^{(1)} = 0.24$, $b_h^{(1)} = 0.51$ when $n_{j0} = 0$, 0.03, 0.05, 0.08 with $n_{i0} = 0.83$, 0.86, 0.88, 0.91

determining whether the solitons are compressive or rarefactive.

Figure 3 shows the Sagdeev potential function $\psi(\phi)$ against ϕ for the large-amplitude ion-acoustic fast mode compressive solitons under the variation of the temperatures of positive (σ_i) and negative (σ_j) ions for $n_{j0} = 0.05$, $n_{i0} = 0.88$, $\chi = 0.17$, $u_{i0} = 0.4$, $u_{j0} = 0.2$; $\sigma_p = 0.41$, $Z = 1$, $\beta_1 = 0.25$, $\mu = = 0.15$, $\nu = 0.85$, $b_l = 0.15$, $b_h = 0.4$, $b_l^{(1)} = 0.24$, $b_h^{(1)} = 0.51$, $V = 1.6$ when $\sigma_i = \frac{1}{100}$, $\sigma_j = \frac{1}{20}$; $\sigma_i = \frac{1}{40}$, $\sigma_j = \frac{1}{50}$; $\sigma_i = \frac{1}{30}$, $\sigma_j = \frac{1}{20}$; $\sigma_i = \frac{1}{20}$, $\sigma_j = \frac{1}{30}$ denoted respectively by the curves c_1, c_2, c_3, and c_4. All these curves represent the exact solitonic nature. It is observed from this figure that the amplitudes are increasing (or reducing) when the temperatures of both positive and negative ions are decreasing (or increasing). It is further mentioned that no solitary waves are formed, when $\sigma_i = 0$, $\sigma_j = 0$ for the above plasma parameters.

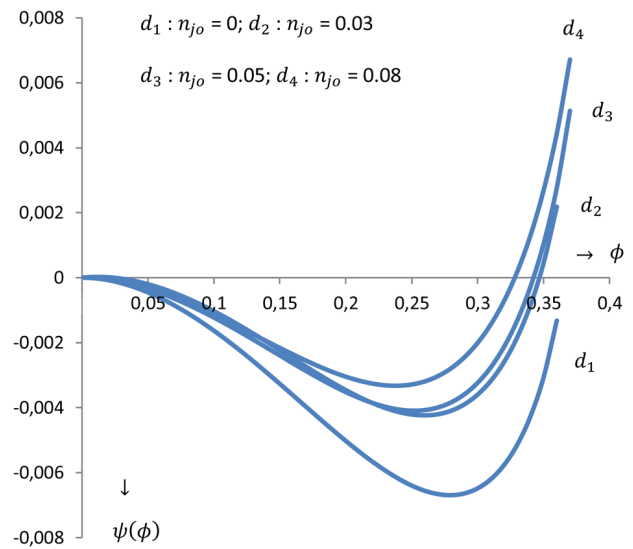The temperatures of positive and negative ions significantly influence the properties of the large-amplitude fast mode compressive solitons. Generally the increase of positive and negative ion temperatures reduce the amplitude and broaden the width of the compressive solitons. Again higher ion temperatures contribute to an increase in the soliton speed. This is because increased thermal motion enhances the effective sound speed in the plasma. The range of Mach numbers for the fast mode solitons is influenced by ion temperatures. Higher temperatures tend to narrow the permissible range, potentially destabilizing the solitons at extreme values. Moreover, temperatures modify the balance between nonlinearity and dispersion. Specifically, higher temperatures enhance dispersive effects, which can reduce the nonlinearity required to form stable solitons.

In Fig. 4, the Sagdeev potential function $\psi(\phi)$ against ϕ for the large-amplitude ion-acoustic fast mode compressive solitons are shown under the variation of the negative ion concentrations (n_{j0}) for $\sigma_i = \frac{1}{30}$, $\sigma_j = \frac{1}{20}$, $\chi = 0.17$, $u_{i0} = 0.4$, $u_{j0} = 0.2$; $\sigma_p = 0.41$, $Z = 1$, $\beta_1 = 0.25$, $\mu = 0.15$, $\nu = 0.85$, $b_l = 0.15$, $b_h = 0.4$, $b_l^{(1)} = 0.24$, $b_h^{(1)} = 0.51$, $V = 1.6$, when $n_{j0} = 0$, 0.03, 0.05, 0.08 with $n_{i0} = 0.83$,
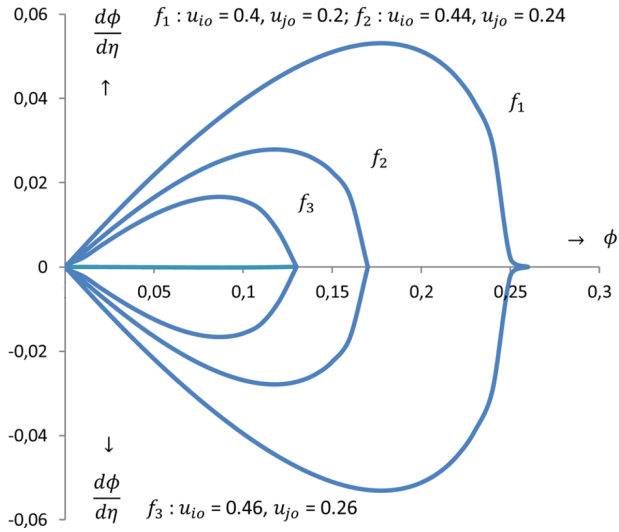
Fig. 5. Profiles of the fast mode phase plane trajectories $\left(\frac{d\phi}{d\eta}\right)$ of compressive solitons in two-temperature nonisothermal electron plasmas against the electrostatic potential (ϕ) under the variation of the stream velocities of positive (u_{i0}) and negative (u_{j0}) ions for $\sigma_i = \frac{1}{30}$, $\sigma_j = \frac{1}{20}$, $\chi = 0.17$, $n_{j0} = 0.05$, $n_{i0} = 0.88$, $\sigma_p = 0.41$, $Z = 1$, $\beta_1 = 0.25$, $\mu = 0.15$, $\nu = 0.85$, $b_l = 0.15$, $b_h = 0.4$, $b_l^{(1)} = 0.24$, $b_h^{(1)} = 0.51$, $V = 1.55$, when $u_{i0} = 0.4$, $u_{j0} = 0.2$; $u_{i0} = 0.44$, $u_{j0} = 0.24$; $u_{i0} = 0.46$, $u_{j0} = 0.26$

0.86, 0.88, 0.91 represented by the curves d_1, d_2, d_3, and d_4 respectively. Of these four curves, only d_3 for $n_{j0} = 0.05$ and d_4 for $n_{j0} = 0.08$ represent the exact solitonic nature whereas the curves d_1 for $n_{j0} = 0$ and d_2 for $n_{j0} = 0.03$ do not show such nature. It is also seen from our observation that the amplitudes of the solitons decrease, when negative ion concentration increases.

Increase in negative ion concentration leads to a decrease in the amplitude and an increase in the width of compressive solitons. This is because a higher concentration of negative ions enhances the overall shielding effect, reducing the effective nonlinearity needed for compression. Conversely, a lower concentration of negative ions allows for steeper and more localized solitons due to reduced shielding and enhanced nonlinearity. A critical concentration threshold exists for negative ions, beyond which compressive solitons might transition to rarefactive solitons, or the solitons may not form at all. Increasing negative ion concentration typically decreases the soliton speed because it lowers the effective sound speed by increasing the overall mass density in the plasma. Again,

higher concentration of negative ions enhance the dispersive effects, which can reduce the nonlinearity required for soliton formation. This balance is crucial for maintaining the stability of the large-amplitude solitons. Moreover, the permissible range of Mach numbers for the existence of the fast mode solitons is influenced by negative ion concentrations. Higher concentrations generally narrow this range, making the solitons more sensitive to perturbations. In addition to this, the negative ion concentration alters the equilibrium of positron and electron densities due to the requirement of overall charge neutrality, indirectly affecting the plasma frequency and soliton characteristics.

We are now discussing the fast mode phase plane trajectories $\left(\frac{d\phi}{d\eta}\right)$ of compressive solitons against the electrostatic potential (ϕ) in two-temperature nonisothermal electron plasmas under the variation of some plasma parameters.

Figure 5 shows the profiles of the fast mode phase plane trajectories $\left(\frac{d\phi}{d\eta}\right)$ of compressive solitons in two-temperature nonisothermal electron plasmas against the electrostatic potential (ϕ) under the variation of the stream velocities of positive (u_{i0}) and negative (u_{j0}) ions for $\sigma_i = \frac{1}{30}$, $\sigma_j = \frac{1}{20}$, $\chi = 0.17$, $n_{j0} = 0.05$, $n_{i0} = 0.88$, $\sigma_p = 0.41$, $Z = 1$, $\beta_1 = 0.25$, $\mu = 0.15$, $\nu = 0.85$, $b_l = 0.15$, $b_h = 0.4$, $b_l^{(1)} = 0.24$, $b_h^{(1)} = 0.51$, $V = 1.55$, when $u_{i0} = 0.4$, $u_{j0} = 0.2$; $u_{i0} = 0.44$, $u_{j0} = 0.24$; $u_{i0} = 0.46$, $u_{j0} = 0.26$ denoted respectively by the curves f_1, f_2, and f_3.

The streaming motions introduce Doppler shifts in the wave frequencies, leading to modifications in the dispersion relation of the fast modes. This affects the phase velocity and trajectory patterns in the phase plane. On the other hand, if the ion streams (u_{i0}, u_{j0}) have velocities close to or exceeding the phase velocity $(V = V_F)$ of the fast mode, resonant interactions can lead to wave amplification or damping and this modifies the phase space trajectories by either steepening or smoothing wave structures. Again, the presence of streaming ions can induce bifurcations in the phase space, altering the equilibrium points of the system. This can lead to new attractors in the phase plane, affecting the long-term behaviour of plasma waves. The interplay between warm ion streaming and wave propagation alters phase plane structures by modifying the energy landscape. It influences separatrix formation, affecting the transition between
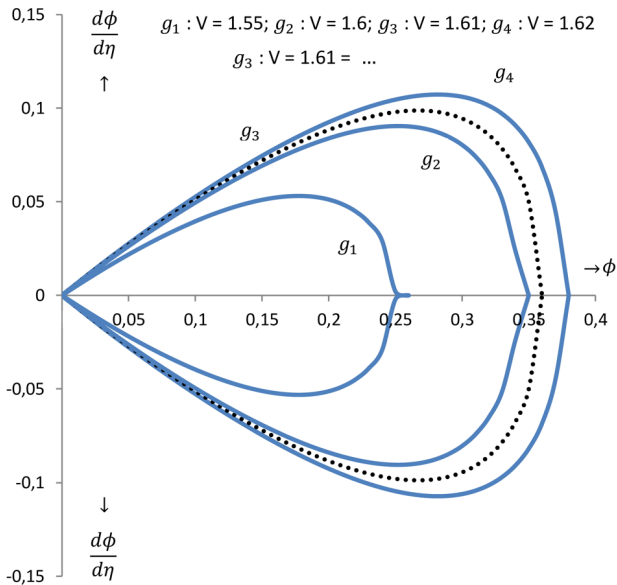
Fig. 6. Profiles of the fast mode phase plane trajectories $\left(\frac{d\phi}{d\eta}\right)$ of compressive solitons in two-temperature nonisothermal electron plasmas against the electrostatic potential (ϕ) under the variation of the phase velocity (V) for $\sigma_i = \frac{1}{30}$, $\sigma_j = \frac{1}{20}$, $\chi = 0.17$, $n_{j0} = 0.05$, $n_{i0} = 0.88$, $\sigma_p = 0.41$, $Z = 1$, $\beta_1 = 0.25$, $\mu = 0.15$, $\nu = 0.85$, $b_l = 0.15$, $b_h = 0.4$, $b_l^{(1)} = 0.24$, $b_h^{(1)} = 0.51$, $u_{i0} = 0.4$, $u_{j0} = 0.2$ when $V = 1.55, 1.6, 1.61, 1.62$.

stable and unstable regions. In space plasmas, fast mode waves interact with streaming ions, affecting energy transport and particle acceleration.

In Fig. 6, the profiles of the fast mode phase plane trajectories $\left(\frac{d\phi}{d\eta}\right)$ of compressive solitons in two-temperature nonisothermal electron plasmas against the electrostatic potential (ϕ) under the variation of the phase velocities (V) for $\sigma_i = \frac{1}{30}$, $\sigma_j = \frac{1}{20}$, $\chi = 0.17$, $n_{j0} = 0.05$, $n_{i0} = 0.88$, $\sigma_p = 0.41$, $Z = 1$, $\beta_1 = 0.25$, $\mu = 0.15$, $\nu = 0.85$, $b_l = 0.15$, $b_h = 0.4$, $b_l^{(1)} = 0.24$, $b_h^{(1)} = 0.51$, $u_{i0} = 0.4$, $u_{j0} = 0.2$, when $V = 1.55, 1.6, 1.61, 1.62$ represented by the curves g_1, g_2, g_3, and g_4 respectively.

The fast mode corresponds to a higher V, altering the effective potential structure in the phase plane. As V increases, the width and depth of the potential well change, affecting the oscillatory nature of trapped particles in the wave. Large V results in wider separatrices in the phase plane, allowing larger amplitude oscillations. The phase velocity V has profound effects on the large-amplitude fast mode phase
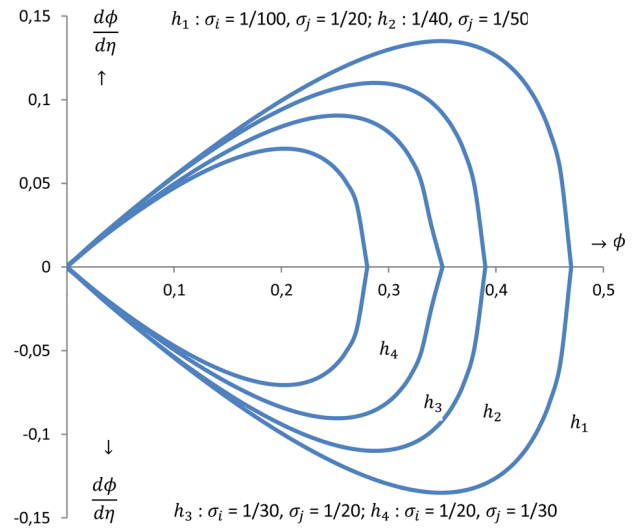

Fig. 7. Profiles of the fast mode phase plane trajectories of compressive solitons in two-temperature nonisothermal electron plasmas are shown under the variation of the temperatures of positive (σ_i) and negative (σ_j) ions for $n_{j0} = 0.05$, $n_{i0} = 0.88$, $\chi = 0.17$, $V = 1.6$, $u_{i0} = 0.4$, $u_{j0} = 0.2$, $\sigma_p = 0.41$, $Z = 1$, $\beta_1 = 0.25$, $Q = 1.9$, $\mu = 0.15$, $\nu = 0.85$, $b_l = 0.15$, $b_h = 0.4$, $b_l^{(1)} = 0.24$, $b_h^{(1)} = 0.51$ when $\sigma_i = \frac{1}{100}$, $\sigma_j = \frac{1}{20}$; $\sigma_i = \frac{1}{40}$, $\sigma_j = \frac{1}{50}$; $\sigma_i = \frac{1}{30}$, $\sigma_j = \frac{1}{20}$; $\sigma_i = \frac{1}{20}$, $\sigma_j = \frac{1}{30}$.

plane trajectories, influencing wave steepening, particle trapping and wave stability. These effects have applications in space physics, fusion research, laboratory plasma experiments, particle acceleration and plasma propulsion systems, making them critical in both theoretical and applied plasma physics.

In Fig. 7, the profiles of the fast mode phase plane trajectories $\left(\frac{d\phi}{d\eta}\right)$ of compressive solitons in two-temperature nonisothermal electron plasmas against the electrostatic potential (ϕ) are shown under the variation of the temperatures of positive (σ_i) and negative (σ_j) ions for $n_{j0} = 0.05$, $n_{i0} = 0.88$, $\chi = 0.17$, $V = 1.6$, $\sigma_p = 0.41$, $Z = 1$, $\beta_1 = 0.25$, $\mu = 0.15$, $\nu = 0.85$, $b_l = 0.15$, $b_h = 0.4$, $b_l^{(1)} = 0.24$, $b_h^{(1)} = 0.51$, $u_{i0} = 0.4$, $u_{j0} = 0.2$ when $\sigma_i = \frac{1}{100}$, $\sigma_j = \frac{1}{20}$; $\sigma_i = \frac{1}{40}$, $\sigma_j = \frac{1}{50}$; $\sigma_i = \frac{1}{30}$, $\sigma_j = \frac{1}{20}$; $\sigma_i = \frac{1}{20}$, $\sigma_j = \frac{1}{30}$ denoted respectively by the curves h_1, h_2, h_3, and h_4.

The phase plane of fast mode solitons typically involves velocity and potential (or density perturbations). Higher ion temperatures cause more extended orbits in phase space, reflecting increased wave dispersion. If temperature of positive ion $\sigma_i \neq$ temperature of negative ion σ_j, asymmetries appear in the
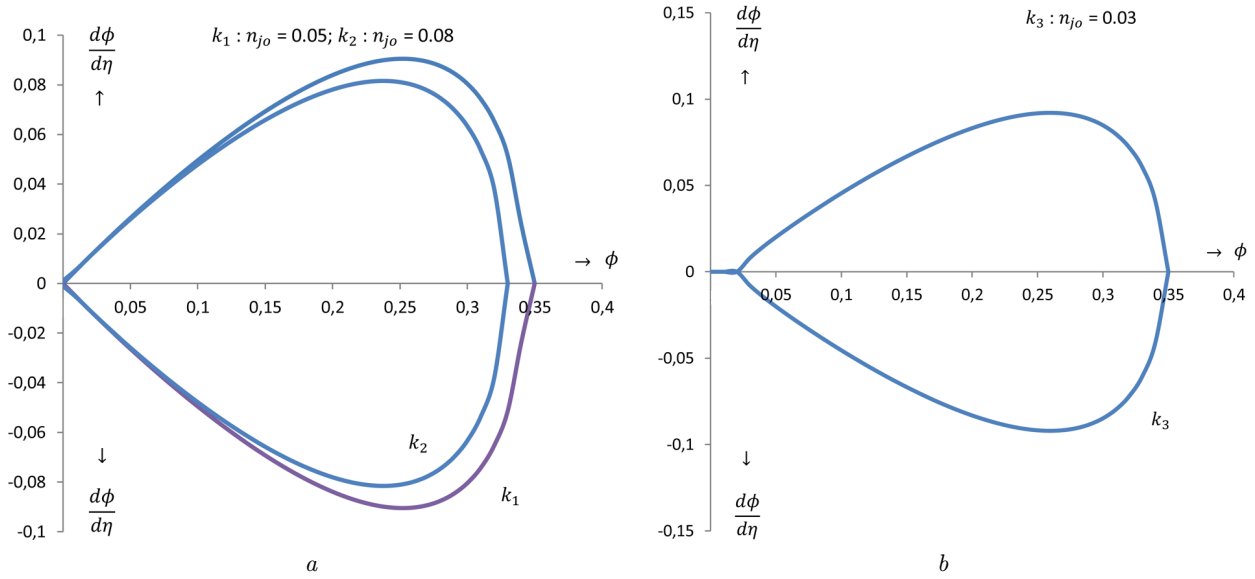
Fig. 8. Profiles of the fast mode phase plane trajectories $\left(\frac{d\phi}{d\eta}\right)$ of compressive solitons in two-temperature nonisothermal electron plasmas against the electrostatic potential (ϕ) under the variation of the concentrations of negative ions (n_{j0}) for: $a - \sigma_i = \frac{1}{30}$, $\sigma_j = \frac{1}{20}$, $\chi = 0.17$, $V = 1.6$, $\sigma_p = 0.41$, $Z = 1$, $\beta_1 = 0.25$, $\mu = 0.15$, $\nu = 0.85$, $b_l = 0.15$, $b_h = 0.4$, $b_l^{(1)} = 0.24$, $b_h^{(1)} = 0.51$, $u_{i0} = 0.4$, $u_{j0} = 0.2$ when $n_{j0} = 0.05, 0.08$ with $n_{i0} = 0.88, 0.91$; $b - \sigma_i = \frac{1}{30}$, $\sigma_j = \frac{1}{20}$, $\chi = 0.17$, $V = 1.6$, $\sigma_p = 0.41$, $Z = 1$, $\beta_1 = 0.25$, $\mu = 0.15$, $\nu = 0.85$, $b_l = 0.15$, $b_h = 0.4$, $b_l^{(1)} = 0.24$, $b_h^{(1)} = 0.51$, $u_{i0} = 0.4$, $u_{j0} = 0.2$ when $n_{j0} = 0.03$ with $n_{i0} = 0.86$

trajectories, indicating differential heating effects on soliton stability. When both ion species have high temperatures, the phase plane trajectories tend to become more oscillatory and solitary wave solutions may transition toward shock-like structures. If $\sigma_i > \sigma_j$, the soliton phase velocity increases and the wave form becomes sharper. On the other hand, if $\sigma_i < \sigma_j$, the increased dispersion weakens soliton amplitude and broadens the wave form. If $\sigma_i \approx \sigma_j$, a balance is maintained and the fast mode solitons exhibit stable phase plane trajectories with well defined amplitudes. Thus, the temperatures of positive and negative ions significantly shape the nature of the fast mode solitons, influencing their speed, width, stability and phase space evolution. These effects have broad applications in space physics, fusion energy, plasma propulsion and industrial technologies, making them critical for advancing plasma-based applications today.

Fig. 8, a shows the profiles of the fast mode phase plane trajectories $\left(\frac{d\phi}{d\eta}\right)$ of compressive solitons in two-temperature nonisothermal electron plasmas against the electrostatic potential (ϕ) under the variation of the concentrations of negative ions (n_{j0}) for $\sigma_i = \frac{1}{30}$,

$\sigma_j = \frac{1}{20}$, $\chi = 0.17$, $V = 1.6$, $\sigma_p = 0.41$, $Z = 1$, $\beta_1 = 0.25$, $\mu = 0.15$, $\nu = 0.85$, $b_l = 0.15$, $b_h = 0.4$, $b_l^{(1)} = 0.24$, $b_h^{(1)} = 0.51$, $u_{i0} = 0.4$, $u_{j0} = 0.2$ when $n_{j0} = 0.05, 0.08$ with $n_{i0} = 0.88, 0.91$ represented by the curves k_1 and k_2 respectively.

In Fig. 8, b, the profile of the fast mode phase plane trajectory $\left(\frac{d\phi}{d\eta}\right)$ of compressive solitons in two-temperature nonisothermal electron plasmas against the electrostatic potential (ϕ) is shown under the variation of the concentration of negative ions (n_{j0}) for $\sigma_i = \frac{1}{30}$, $\sigma_j = \frac{1}{20}$, $\chi = 0.17$, $V = 1.6$, $\sigma_p = 0.41$, $Z = 1$, $\beta_1 = 0.25$, $\mu = 0.15$, $\nu = 0.85$, $b_l = 0.15$, $b_h = 0.4$, $b_l^{(1)} = 0.24$, $b_h^{(1)} = 0.51$, $u_{i0} = 0.4$, $u_{j0} = 0.2$ when $n_{j0} = 0.03$ with $n_{i0} = 0.86$ denoted by the curve k_3.

In plasma dynamics, negative ions play a vital regulatory role. Their presence modifies phase trajectories, alters the Sagdeev potential landscape and can lead to a diverse set of nonlinear structures including solitons, supersolitons *etc.* The presence of more negative ion concentrations in a non-isothermal plasma leads to richer fast mode phase plane dynamics, affecting stability, energy transport and nonlinear wave structures. These effects have critical implications in

astrophysics, fusion research, space propulsion and plasma technology. Understanding these conditions enables better control of plasma behaviour in both natural and laboratory settings.

5. Conclusions

We have investigated the ion-acoustic large-amplitude fast mode compressive solitons and the fast mode phase plane trajectories of the bounded periodic solutions of solitary waves in two-temperature nonisothermal electron plasmas under the variation of the streaming motions of positive and negative ions, the different values of the phase velocity V, the temperatures of positive and negative ions and the concentrations of negative ions. The large-amplitude fast mode compressive solitons are observed in the Figs. 1 to 4 and the fast mode phase plane trajectories are represented by the Figs. 5 to 8.

The streaming velocities of both ion species contribute to wave sharpening, leading to an enhancement in soliton amplitude and the emergence of the large-amplitude fast mode compressive solitons. Moreover, the presence of warm positrons modifies the soliton amplitude and width due to their lighter mass and higher mobility. Increasing values of streaming velocities of both positive and negative ions alter phase plane trajectories. In space plasmas, such as the solar wind and magnetospheric environments, fast-mode waves interact with streaming ions, affecting energy transport and particle acceleration. In controlled fusion devices, understanding the fast-mode waves in the presence of streaming ions is critical for optimizing plasma heating and confinement. In pair-ion and dusty plasmas, streaming ions contribute to new wave modes and instabilities, impacting applications in plasma propulsion and space weather modeling.

The effect of phase velocity (V) on soliton profiles determines soliton width and speed, on phase plane trajectories it controls orbit trapping.

Higher ion temperatures tend to broaden the solitons and reduce their amplitude, whereas lower temperatures enhance the nonlinearity. But the phase plane trajectories modify the orbit separatrices for increasing or decreasing values of the temperatures of positive and negative ions.

The concentration of negative ions affects the nonlinear co-efficient and the dispersive properties, modifying soliton stability. The increasing concentration of negative ions shifts the phase plane structure and modifies the potential well depth.

In general, higher streaming velocities and lower temperatures favor the formation of strong solitons, while higher phase velocity alters phase plane trajectories.

The applications of fast-mode large-amplitude solitons and fast-mode phase plane trajectories are primarily found in space and astrophysical plasmas, as well as in laboratory plasma experiments and advanced plasma-based technologies. Large-amplitude fast-mode solitons can help one in understanding shock formation and the dynamics of relativistic plasmas around pulsars and active galactic nuclei. Again, phase plane trajectories are used to analyze the stability of plasma waves and structures, contributing to the design of stable plasma confinement systems and chaotic behaviour of plasma systems. Moreover, nonlinear plasma wave structures are explored for communication in space plasmas and advanced signal processing techniques.

From this paper, the following new results are found:

(i) Existence and Stability: Fast-mode solitons exist as stable nonlinear wave solutions under specific parameter conditions, governed by the underlying plasma or nonlinear wave equations. It is also helpful to analyze how the system parameters affect the amplitude, width and speed of the solitons. In our plasma model, it is mentioned that the fast-mode solitons cannot exist for $V_F < 1.48$ and $V_F > 1.62$ but the stable structure of fast mode solitons exist only in our model plasma for $1.48 \leq V_F \leq 1.62$ where V_F is the phase velocity of fast-mode soliton and satisfies the inequality (14). It is further mentioned that the solitonic nature is also found even if $V = V_F = 1.3$ for $n_{j0} = 0.05$, $n_{i0} = 0.88$, $\sigma_i = \frac{1}{30}$, $\sigma_j = \frac{1}{20}$, $\chi = 0.17$, $\sigma_p = 0.41$, $Z = 1$, $\beta_1 = 0.25$, $\mu = 0.15$, $\nu = 0.85$, $b_l = 0.15$, $b_h = 0.4$, $b_l^{(1)} = 0.24$, $b_h^{(1)} = 0.51$ when $u_{i0} = 0.07$, $u_{j0} = 0.09$ and this is possible due to high stream velocities of positive and negative ions and these arbitrarily chosen set of plasma parameters also satisfy inequality (14) and charge neutrality condition.

(ii) Phase Plane behavior: The phase plane trajectories exhibit distinct patterns depending on the system's initial conditions and governing nonlinearities. These trajectories effectively illustrate the dy-

namical evolution of solitons and their stability properties. From the phase portraits, one can identify the fixed points, separatrix structures and existence domains of fast mode solitons in our model plasma.

(iii) Analytical and Numerical correction: The results, obtained through both analytical techniques and numerical simulations, show strong agreement, confirming the robustness of the derived soliton solutions.

(iv) Physical Implications: The study of fast mode solitons is relevant for various physical contexts, including space plasmas, optical waveguides, laboratory plasmas and hydrodynamic flows, where similar nonlinear wave phenomena are observed.

Thus the results obtained from this two-temperature nonisothermal electron plasmas comprising of warm negative ions, warm positive ions and warm positrons are most probably a new one and attractive.

The future plan of the author is to find the large-amplitude compressive fast mode solitary waves in a magnetized plasma consisting of warm adiabatic positive ions, warm adiabatic negative ions, warm nonisothermal positrons and two-temperature non-isothermal electrons by the Sagdeev pseudopotential method.

1. M.Q. Tran. Propagation of solitary waves in a two ion species plasma with finite ion temperature. *Plasma Physics* **16**, 1167 (1974).

2. M.K. Mishra, R.S.Tiwari, J.K. Chawla. Ion-acoustic solitons in a negative ion plasma with two-electyron temperature distributions. *Phys. Plasmas* **19**, 062303 (2012).

3. Y. Nakamura, H. Bailung, R. Ichiki. Effects of a slow ion beam on ion-acoustic waves. *Phys. Plasmas* **11**, 3795 (2004).

4. M.K. Mishra, R.S. Chhabra. Ion-acoustic compressive and rarefactive solitons in a warm multicomponent plasma with negative ions. *Phys. Plasmas* **3 (12)**, 4446 (1996).

5. A. Paul, A. Bandyopadhyay. Nonlinear fast-mode waves in a two-temperature electron-positron-ion plasma. *Astrophysics and Space Science*, **368** (3), 23 (2023).

6. S. Mahmood, H. Ur-Rehman. Compressive and rarefactive solitons for Fast and Slow ion acoustic waves in multi-ion plasmas. *J. Physical Soc. Jpn.* **82**, 7, (2013).

7. S.N. Paul, C. Das, I. Paul, B. Bandyopadhyay, S. Chattopadhyay, S.S. De. Ion-acoustic solitary waves in an electron-ion-positron plasma. *Indian J. Phys.* **86**, 545 (2012).

8. D.K. Singh, H.K. Malik. Solitons in inhomogeneous magnetized negative ion containing plasma with two-temperature nonisothermal electrons. *IEEE Transactions on Plasma Science* **36** (2), 462 (2008).

9. R.Z. Sagdeev. Cooperative phenomena and shock waves in collisionless plasmas. *Reviews of Plasma Phys.*, Edited by M.A. Leontovich (Consultants Bureau) **4**, 23 (1966).

10. J.L. Cooney, M.T.Gavin, K.E. Lonngren. Experiments on Korteweg-de Vries solitons in a positive ion – negative ion plasma. *Phys. Fluids B* **3** (10), 2758 (1991).

11. F. Verheest, S.R. Pillay. Large-amplitude Fast-mode solitons and double layers in multi-component plasmas. *J. Plasma Phys.* **74** (5), 639 (2008).

12. S. Baboolal, R. Bharuthram, M.A. Hellberg. Cut-off conditions and existence domains for large amplitude ion-acoustic solitons and double layers in fluid plasmas. *J. Plasma Phys.* **44** 1, 1 (1990).

13. G.S. Lakhina, S.V. Singh, A.P. Kakad. Ion-acoustic solitons/double layers in two-ion plasma. *Phys. Plasmas* **21**, 062311 (2014).

14. H. Schamel, V.I. Maslov. Adiabatic growth of electron holes in current-carrying plasmas. *Physica Scripta T* **50**, 42 (1994).

15. H. Schamel, V. Maslov. Langmuir wave contraction caused by electron holes. *Physica Scripta T* **82**, 122 (1999)

16. V. Maslov, H. Schamel. Growing electron holes in drifting plasmas. *Phys. Lette. A* **178** (1–2), 171 (1993).

17. V.I. Maslov. Electron beam excitation of a potential well in a magnetized plasma waveguide. *Phys. Lett. A* **165** (1), 63 (1992).

18. S.G. Tagare. Effect of ion temperature on ion-acoustic solitons in a two-ion warm plasma with adiabatic positive and negative ions and isothermal electrons. *J. Plasma Phys.* **36**, 301 (1986).

19. F. Verheest. Ion-acoustic solitons in multi-component plasmas including negative ions at critical densities. *J. Plasma Phys.* **39**, 71 (1988).

20. K.P. Das, F. Verheest. Ion-acoustic solitons in magnetized multi-component plasmas including negative ions. *J.Plasma Phys.* **41**, 139 (1989).

21. M.K. Mishra, R.S. Chhabra, S.R. Sharma. Obliquely propagating ion-acoustic solitons in a multi-component magnetized plasma with negative ions. *J. Plasma Phys.* **52** (3), 409 (1994).

22. G.S. Lakhina, S.V. Singh, A.P. Kakad, F. Verheest, R. Bharuthram. Study of nonlinear ion- and electron-acoustic waves in multi-component space plasmas. *Nonlinear Processes in Geophysics* **15**, 903 (2008).

23. S.K. Maharaj, R. Bharuthram, S.V. Singh, G.S. Lakhina. Existence domains of arbitrary amplitude nonlinear structures in two-electron temperature space plasmas. *Phys. Plasmas* **21** (19), 122301 (2012).

24. M.A. Hellberg, F. Verheest. Ion-acoustic solitons in plasmas with two-temperature ions. *Phys. Plasmas* **15**, 062307 (2008).

25. F. Verheest, M.A. Hellberg. Ion-acoustic solitons in plasma with two adiabatic constituents. *J. Plasma Phys.* **76** (3–4), 277 (2010).

26. F. Nsengiyumva, M.A. Hellberg, F. Verheest, R.L. Mace. Stopbands in the existence domains of acoustic solitons. *Phys. Plasmas* **21**, 102301 (2014).

27. S.K. Maharaj, R. Bharuthram, S.V. Singh, G.S. Lakhina. Existence domains of slow and fast ion-acoustic solitons in two-ion space plasmas. *Phys. Plasmas* **22**, 032313 (2015).

28. S. Sebastian, M. Michael, G. Sreekala, A. Varghese, V. Chandu. Fast and slow mode solitary waves in a five-component plasma. *Brazilian J. Phys.* **47** (1), 46 (2017).

29. G.S. Lakhina, S.V. Singh, R. Rubia, S. Devanandhan. Electrostatic solitary structures in space plasmas: Soliton perspective/plasma. *MDPI J./Plasma* **4** (4), 681 (2021).

30. H. Malik, K. Singh. Small amplitude soliton propagation in a weakly relativistic magnetized space plasma: Electron inertia contribution. *IEEE Trans. Plasma Sci.* **33** (6), 1995 (2005).

31. S. Chattopadhyay. Existence of small-amplitude double layers in two-temperature nonisothermal plasma. *Ukr. J. Phys.* **68** (12), 795 (2023).

32. X. Mushinzimana, F. Nsengiyumva. Large amplitude slow ion-acoustic solitary waves in a warm negative ion plasma with superthermal electrons: The fast mode revisited, AIP Advances **10** (6), 065305 (2020).

33. Rajkumar Roychoudhury. Quasipotential approach to solitary wave solutions in nonlinear plasma. *Proc. Inst. of Math. NAS of Ukraine* **30** (2), 510 (2000).

34. G.O. Ludwig, J.L. Ferreira, Y. Nakamura. Observation of ion-acoustic rarefaction solitons in a multicomponent plasma with negative ions. *Phys. Rev. Lett.* **52** (4), 275 (1984).

35. B. Song, N. D'Angelo and R.L.Merlino. Ion-acoustic waves in a plasma with negative ions. *Phys. Fluids B* **3**, 284 (1991).

36. B. Handique, H. Bailung, G.C. Das, J. Chutia. Observations of low-frequency mode in a multicomponent plasma with negative ions. *Phys. Plasmas* **6**, 1636 (1999).

37. R. Ichiki, S. Yoshimura, T. Watanabe, Y. Nakamura, Y. Kawai. Experimental observation of dominant propagation of the ion-acoustic slow mode in a negative plasma and its application. *Phys. Plasmas* **9**, 4481 (2002).

38. C.P. Olivier, S.K. Maharaj, R. Bharuthram. Ion-acoustic solitons, double layers and supersolitons in a plasma with two ion and two electron species. *Phys. Plasmas* **22**, 082312 (2015).

39. G.S. Lakhina, S. Singh, R. Rubia, S. Devanandhan. Electrostatic solitary structures in space plasmas: Soliton perspective. *MDPI J. Plasma* **4** (4), 681 (2021).

40. F. Verheest, M.A. Hellberg, I. Kourakis. Acoustic solitary waves in dusty and/or multi-ion plasmas with cold, adiabatic and hot constituents. Phys. Plasmas 15, 112309 (2008).

41. F. Verheest, M.A. Hellberg, G.S. Lakhina. Necessary conditions for the generation of acoustic solitons in magnetospheric and space plasmas with hot ions. *Astrophys. Space Sci. Trans.* **3**, 15 (2007).

42. S. Chattopadhyay. Effects of ionic temperatures on phase velocities of ion-acoustic solitary waves in a drift negative ion plasma with single temperature electron. *FIZIKA A* (Zagreb) **16** (1), 25 (2007).

43. S.G. Tagare, R. Virupakshi Reddy. Effect of ionic temperature on ion-acoustic solitons in a two-ion warm plasma consisting of negative ions and nonisothermal electrons. *Plasma Phys. Controlled Fusion* **29** (6), 671 (1987).

44. R. Virupakshi Reddy, S.G. Tagare. Effect of ionic temperatures on ion-acoustic solitons in a two-electron-temperature plasma with adiabatic positive and negative ions and isothermal electrons. *J. Physical Soc. Jpn.* **56** (12), 4329 (1987).

45. S.G. Tagare, R.V. Reddy. Effect of higher-order nonlinearity on propagation of nonlinear ion-acoustic waves in a collisionless plasma consisting of negative ions. *J. Plasma Phys.* **35**, 219 (1986).

46. S. Chattopadhyay. Effects of drift negative ion plasmas on ion-acoustic solitary waves in drift cold positive ion plasmas with isothermal electrons. *Fizika A (Zagreb)* **16** (2), 63 (2007).

С. Чаттопадхай

ШВИДКІ ІОН-АКУСТИЧНІ
СОЛІТОННІ ХВИЛІ В ГАРЯЧІЙ ПЛАЗМІ ВІД'ЄМНО
ЗАРЯДЖЕНИХ ІОНІВ З ДВОТЕМПЕРАТУРНИМИ
НЕІЗОТЕРМІЧНИМИ ЕЛЕКТРОНАМИ

Використовуючи формалізм псевдопотенціалу Сагдеєва, було проведено дослідження іонно-акустичних швидких солітонів великої амплітуди та їх траєкторій на фазовій площині для модельної плазми, яка складається з гарячих позитивних і негативних іонів, гарячих позитронів та двотемпературних неізотермічних електронів. Критична фазова швидкість (V_c) спочатку отримується аналітично шляхом розв'язання дисперсійного співвідношення за різних фізичних умов. На основі цього аналізу фазова швидкість згодом ідентифікується як швидкість, яка не тільки перевищує критичне значення, але й задовольняє критерії існування солітонних розв'язків включно із усіма необхідними граничними умовами.

К л ю ч о в і с л о в а: фазова швидкість, швидкі солітони, двотемпературна неізотермічна електронна плазма, ізотермічні позитрони, траєкторії на фазовій площині.